Analyst

CRITICAL REVIEW

View Article Online
View Journal | View Issue

Cite this: *Analyst*, 2026, **151**, 1567

PFAS isomers in aquatic biota: revealing differences in occurrence, bioaccumulation, and biotransformation through isomer-specific analysis

Mindula K. Wijayahena [a] and Diana S. Aga *[a,b]

Historical production of per- and polyfluoroalkyl substances (PFAS) *via* electrochemical fluorination has resulted in complex mixtures of linear (L) and branched (Br) isomers, yet most environmental studies still treat them as single compounds. Emerging research highlights that isomer-specific differences critically shape PFAS environmental fate, bioaccumulation, and toxicity. These distinctions are particularly critical for aquatic organisms, which experience continuous exposure to PFAS and serve as sentinels of ecosystem health. A comprehensive review of literature from January 2000 to December 2025 reveals that most studies on PFAS in aquatic species overlook isomer resolution, constraining insights into mixture behavior. The relatively few studies that report isomer profiles across fish, sharks, marine mammals, aquatic insects, seabirds, alligators, and polar bears primarily focus on PFOS (perfluorooctane sulfonic acid), leaving substantial knowledge gaps for other PFAS classes. Evidence also indicates that precursor compositions strongly influence isomer-specific bioaccumulation; several studies show that L-isomers tend to bioaccumulate more than their Br counterparts, suggesting potential differences in environmental stability and metabolism. Advancing knowledge on PFAS isomer distribution requires broader use of orthogonal separation techniques. Ion mobility spectrometry can resolve L- and Br-isomers based on differences in their collision cross-sections. Other techniques that can separate L- and Br-isomers include gas chromatography/mass spectrometry with derivatization, and supercritical fluid chromatography/mass spectrometry, capable of efficient separation of isomers based on differences in partition coefficients between two phases. Integrating these techniques into current conventional PFAS analytical methods is essential for uncovering the PFAS structure-environmental behavior and for enhancing future ecological risk assessments.

Received 27th November 2025,
Accepted 24th February 2026

DOI: 10.1039/d5an01246e

rsc.li/analyst

1. Introduction

Global contamination with per- and polyfluoroalkyl substances (PFAS) poses a threat to both human health and the environment.[1] PFAS are a group of synthetic fluorinated chemicals that have been found ubiquitously in the environment, including in water, soil, wildlife, and food.[2,3] Human exposure to PFAS mainly occurs through contaminated drinking water and food sources, with seafood being a significant non-occupational exposure route, which can lead to various negative health issues.[4–8] Seafood consumption provides essential nutrients to the human diet and contributes to global food security.[9] Over the past 60 years, the global per capita consumption of fish has been steadily increasing from 9.1 kg per year to an average of 20.7 kg per year in 2022.[10] However, consumption of PFAS-contaminated seafood has been linked to a range of adverse health outcomes, including various types of cancer,[4] immunotoxicity,[6] thyroid disorders,[5] neurotoxicity,[8] and reduced vaccine response.[7] In the absence of federal regulations for PFAS levels in seafood in the United States (US),[11] several states have established their own guidelines.[12,13]

Fish and wildlife are exposed to PFAS both through their habitats, such as contaminated waterways,[14] and through their diets.[15] Hundreds of studies have reported PFAS accumulation across a wide range of species and geographic regions,[16] as illustrated by the Environmental Working Group's (EWG) global map of PFAS contamination in wildlife, which compiles data from more than 125 peer-reviewed studies.[17] A recent study using histopathology and gene transcript analyses in fish found that PFAS exposure is linked to inflammation, oxidative stress, endocrine disruption, and altered immune path-

[a]*Department of Chemistry, University at Buffalo, The State University of New York, Buffalo, NY 14260, USA. E-mail: dianaaga@buffalo.edu; Tel: +1 (716) 645-4220*
[b]*Research and Education in Energy, Environment and Water (RENEW) Institute, University at Buffalo, The State University of New York, Buffalo, NY 14260, USA*

ways.[18] Further, EWG has emphasized adverse outcomes associated with PFAS exposure in wildlife, including effects on the immune system, thyroid and endocrine system, nervous system, reproductive system, and cholesterol levels.[1]

Numerous recent reviews have provided insights into the manufacturing and applications of PFAS,[19,20] their global distribution and exposure pathways,[21,22] their bioaccumulation potential, and their associated toxicity.[23,24] This current literature review is focused on the occurrence, bioaccumulation, and biomagnification of PFAS isomers in aquatic species, covering papers published from January 2000 to December 2025. For over five decades of global PFAS production, more than 14 000 distinct chemical structures have been manufactured, each varying in degree of fluorination and containing diverse isomeric impurities.[25] These structural differences can profoundly influence the environmental fate, transport, and bioaccumulation of PFAS. Accordingly, the objective of this comprehensive review is to evaluate the extent to which current ecological monitoring of aquatic biota accounts for isomer-specific variability in PFAS bioaccumulation. By synthesizing available evidence and identifying critical knowledge gaps, this review aims to clarify the most urgent research needs for improving ecological risk assessments and to inform future regulatory and monitoring strategies.

1.1 Overview of linear *vs.* branched PFAS isomers

In the past, PFAS production was primarily carried out through electrochemical fluorination (ECF), a process that yields a mixture of linear (L) and branched (Br) isomers. ECF typically produces approximately 95% L-isomers for perfluorohexane sulfonic acid (PFHxS), 70–80% for perfluorooctane sulfonic acid (PFOS), and 80–85% for perfluorooctanoic acid (PFOA), with the remaining fractions consisting of Br-isomers.[26–29] Additional pathways for introducing PFAS isomers into the environment arise from the biotransformation of precursor PFAS (Pre-PFAS) which can generate different proportions of L- and Br-PFAS.[30,31] Biodegradation of PFAS by certain microorganisms has also been shown to produce by-products consisting of many isomers.[32,33] Lastly, fluorinated polymers are expected to degrade into non-polymeric PFAS, contributing further to the release of Br-PFAS.[34,35] Collectively, these various processes introduce additional PFAS isomers into the environment, affecting the relative distribution between L and Br-isomers.

Both linear (L-PFHxS, L-PFOS, L-PFOA, L-PFAS) and branched (Br-PFHxS, Br-PFOS, Br-PFOA, Br-PFAS) forms are commonly detected in environmental and biological matrices. Differences in production methods and the release of PFAS isomers across different geographic regions and time periods result in varying ratios of L- and Br-PFAS isomers in biotic and abiotic environments.[19] Specific isomer-dependent bioaccumulation patterns have been documented in both humans and animals. In humans, reported ratios of L-PFOS to total-PFOS (T-PFOS) include 49 ± 16% in whole blood,[36] 46 ± 14% in plasma,[36] and 60 ± 10% in serum.[37] Similarly, L-PFHxS is strongly enriched in serum, with L-PFHxS/T-PFHxS ratios of 93.1 ± 3.0% in infants (2–4 months) and 94.3 ± 2.9% in postpartum mothers (3 weeks after delivery).[38] In animals, reported L-PFOS/T-PFOS ratios vary widely, ranging from 33.5 ± 6.5% in fish fillets[39] to more than 88% in avian eggs.[40] Notably, L-PFOA/T-PFOA ratios typically exceed 90% in both humans and animals.[36,40–42] A more detailed discussion of isomer-specific bioaccumulation patterns in aquatic biota is provided in subsequent sections of this review.

The bioaccumulation of PFAS is influenced by hydrophobicity, protein-binding affinity, and molecular size and

Mindula K. Wijayahena

Mindula K. Wijayahena, hailing from Kandy, Sri Lanka, earned her Bachelor of Science in Chemistry from the University of Sri Jayewardenepura in 2019. She is currently a doctoral student under the supervision of Dr Diana S. Aga, Department of Chemistry, University at Buffalo, The State University of New York, Buffalo, NY, United States. Her research primarily focuses on developing extraction and analytical methods for PFAS and PFAS isomer analysis across multiple biological and environmental matrices: blood, fish, and water using liquid chromatography tandem mass spectrometry (LC-MS/MS) and ultra-high-performance LC coupled to cyclic ion mobility separation with time of flight mass spectrometry (UPLC-cIMS-QToF/MS).

Diana S. Aga

Diana S. Aga is a SUNY Distinguished Professor, the Henry Woodburn Professor of Chemistry, and the Director of RENEW Institute (Research and Education in Energy, Environment, and Water) at the University at Buffalo. An expert in analytical and environmental chemistry, she leads pioneering research on the fate, transport, and treatment of chemicals of emerging concern, particularly per- and polyfluoroalkyl substances (PFAS), and other persistent organic pollutants. Through targeted and non-targeted analyses, her work advances understanding of the bioaccumulation, toxicity, and environmental impacts of contaminants in humans and wildlife, and supports the development of innovative treatment technologies to remove contaminants from wastewater.

shape.[43,44] Moreover, beyond differences introduced during synthesis, the environmental behavior of PFAS isomers, including their transport, degradation, and bioaccumulation rates can also influence their relative abundances. Lower concentrations of Br-PFAS in biota are likely due to their lower octanol–water partition coefficients (K_{ow}) compared with their linear counterparts,[45,46] which reduce their propensity for bioaccumulation, particularly in higher trophic level organisms such as cetaceans.

Although both L- and Br-PFAS isomers are ubiquitous in the environment, quantitative analyses still predominantly treat these structural isomers as a single entity, with all isomers commonly co-eluting and integrated into one chromatographic peak.[26] Consequently, environmental monitoring programs frequently report T-PFOS or T-PFOA, without resolving individual isomers. This practice warrants critical reevaluation, as an increasing body of evidence demonstrates that L- and Br-isomers differ in their environmental fate, bioaccumulation behavior, and associations with human health outcomes.[28] Historically, limitations in chromatographic resolution constrained the ability to distinguish isomers and led most studies to focus solely on T-PFOS measurements.[41,47] However, recent advances in instrumentation, including improvements in ultra-performance liquid chromatography (UPLC) systems, coupled with ion mobility spectrometer and a high-resolution mass spectrometer (MS), now allow robust isomer-specific separation and quantification.[39] These developments underscore the importance of transitioning from T-PFAS reporting to isomer-resolved analysis, which is essential for accurately characterizing exposure sources, understanding toxicokinetic variability, and refining ecological and human health risk assessments.

Current regulatory monitoring in the US and Europe for PFOS and PFOA focuses on total isomer concentrations without differentiating between structural forms,[48,49] an approach that merits reconsideration in light of emerging evidence of isomer-specific toxicological profiles.[28] For example, exposure to Br-PFOS has been more strongly associated with altered birth weight,[50] higher prevalence of hypertension,[51] and liver cell injury[52] than L-PFOS. Additional findings link Br-PFOS to impaired renal function.[53] A separate study reported that L-PFOA is significantly associated with increased incidence of visual impairment, a relationship not observed for Br-PFOA.[54] Moreover, both L- and Br-PFOS exhibit positive correlations with total protein and albumin, while elevated L-PFOA levels are associated with increased total cholesterol and albumin, but inversely correlated with globulin concentrations.[55]

1.2 What does this review paper discuss

Seafood is a critical source of dietary protein and livelihoods for populations worldwide. In addition to supplying essential nutrients, fish consumption globally plays an important role in sustaining food security.[9] However, seafood can also serve as a pathway for human exposure to environmental contaminants, including PFAS.[56,57] Recent studies have documented measurable levels of PFAS in fish and other seafood products purchased from U.S. markets.[39,57–59]

This review synthesizes recent advances in the understanding of PFAS isomer behavior in aquatic biota and places these findings in the context of earlier studies. Specifically, the review: (1) examines the occurrence, distribution, bioaccumulation, and biomagnification of L- and Br-PFAS isomers across diverse aquatic organisms, such as fish (including sharks), marine mammals (whales and dolphins), shellfish, polar bears, aquatic insects, seabirds, and alligators; (2) evaluates advancements in extraction and analytical methodologies that enable isomer-specific measurements; and (3) identifies key knowledge gaps and outlines priority areas for future research. Although PFOS and PFOA isomers remain the most extensively studied, this review also incorporates findings on other PFAS isomers. Additionally, we compare environmental patterns of L- and Br-PFAS isomers in biota with those typically produced by ECF, providing insight into potential sources and transformation processes.

2. Methodology of the review paper

A systematic search of the Web of Science database was conducted to identify relevant studies on PFAS isomers in aquatic organisms and seafood products. The search query (https://www.webofscience.com/wos/alldb/summary/ee20c842-5aad-42b4-b7ee-e8a195705cca-019ad2185a/relevance/1) was constructed to capture articles related to both L- and Br-isomers of various PFAS. The following search string was used: TS = (PFAS OR PFOS OR PFOA OR PFHxS OR perfluorooctane sulfonate OR perfluorooctanoic acid OR perfluorohexane sulfonate OR perfluorooctane sulfonic acid OR perfluorohexane sulfonic acid OR perfluoroalkyl OR perfluorinated OR perfluorooctanesulfonate OR perfluorooctanesulfonic OR heptadecafluorooctane sulfonic OR perfluorooctanoate OR perfluorooctane-1-sulfonic acid OR perfluorohexanesulfonate OR perfluorohexanesulfonic OR tridecafluorohexane-1-sulfonic acid OR perfluorohexanoate OR perfluorohexane-1-sulfonic acid OR perfluorooctanecarboxylate OR perfluorooctanecarboxylic OR pentadecafluorooctanoic acid OR pentadecafluoro-1-octanoic acid) AND TS = (isomer OR branched isomer OR linear isomer) AND TS = (fish OR seafood OR aquatic animal OR marine organism OR aquatic organism OR market OR fish fillet). The search included all publication years available in the database from January 2000 to December 2025. Interestingly, the search provided papers only starting from 2008, indicating that earlier studies did not consider distinguishing between any of the isomers. In addition, some relevant studies published during this period, identified through a Google Scholar search and cited in the bibliographies of the initially identified articles, were included in this review. This expanded search strategy led to the inclusion of several additional publications, notably one from 2004, along with a few newly released papers from 2025. Therefore, the papers from Web of Science search, relevant studies identified through Google Scholar searches, cross-referenced from the bibliographies of the initially selected articles, and general Google searches were incorporated into this review.

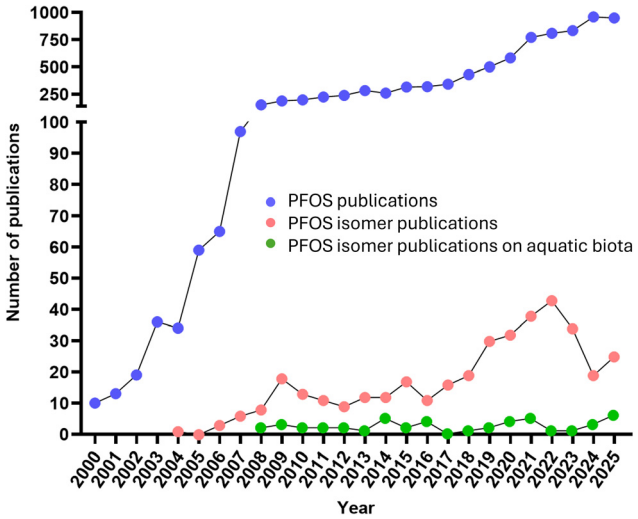

Fig. 1 Publication trends on PFOS, PFOS isomers, and PFOS isomers in aquatic biota from January 2000 to December 2025. The number of publications on PFOS and PFOS isomers are based on Web of Science records. The PFOS isomers in aquatic biota publication number was obtained using all the papers reviewed in the current review paper. Search terms for PFOS included "PFOS" OR "perfluorooctane sulfonic acid", while PFOS isomer searches used "PFOS isomer" OR "PFOS isomers" OR "perfluorooctane sulfonic acid isomer" OR "perfluorooctane sulfonic acid isomers".

To illustrate the trajectory of PFAS isomer research between January 2000 and December 2025, Fig. 1 presents the publication trends on PFOS, PFOS isomers, and PFOS isomers specifically in aquatic biota. PFOS was selected as the focal compound because it is the most frequently detected across nearly all environmental matrices and exhibits a relatively high proportion of structural isomers. As shown in Fig. 1, research on PFOS has expanded rapidly since 2000, reaching approximately 1000 publications per year during the last five years (2021–2025). Interest in PFOS isomers began to emerge around 2004, based on Web of Science searches that did not specify any environmental matrix. However, research specifically examining PFOS isomers in aquatic biota did not appear until 2008, when two studies independently reported isomer-resolved analyses, one investigating zooplankton, mysids, Diporeia, alewife, smelt, sculpin, and lake trout, and the other analyzing zooplankton, Arctic cod, and seals. Since then, the number of studies addressing PFOS isomer profiles in aquatic organisms has increased steadily, although at a slower pace than the broader PFOS literature. To date, only 53 published papers have reported or acknowledged the presence of PFOS isomers in aquatic biota.

3. Approaches for PFAS extraction in aquatic biota

The sample extraction protocols for analyzing PFAS isomers in liquid chromatography mass spectrometry (LC-MS) and gas chromatography mass spectrometry (GC-MS) are primarily optimized for maximum recovery of PFAS from complex matrices rather than for selectively targeting individual isomers. Although not specifically designed for isomer isolation, the efficiency of these methods in extracting a wide range of PFAS allows researchers to subsequently apply them for detailed isomer analysis. As a result, with these extraction procedures, previous studies have examined isomers in various aquatic organisms, including zooplankton, aquatic insects, shellfish, different fish species, polar bears, seabirds, and alligators (Table 1). Sample masses used across the reviewed studies range from 0.1 g to 1 g, depending on the specific method development protocols. Extraction procedures have employed homogenized, freeze-dried samples,[39,60] and some have used samples without freeze-drying.[29,47,61,62] While freeze-drying provides enhanced reproducibility and higher analyte recoveries,[63] this process may lead to the loss of volatile compounds, including PFAS sulfonamide precursors and ethanol-based species. Therefore, it is important to know the physicochemical properties of the analytes of interest when choosing the appropriate sample preparation techniques. To date, the analysis of volatile PFAS remains challenging. A recent study[64] shows that the use of headspace solid-phase microextraction (SPME) or direct immersion SPME can be an effective preconcentration method for volatile or semi-volatile PFAS, such as fluorotelomer alcohols (FTOHs), perfluorooctanesulfonamides (PFOSAs), and a perfluorooctanesulfonamidoethanol (FOSE). However, these preconcentration methods have not been applied in studies that examine isomer separation.

Over the past two decades, various methods have been employed to extract PFAS and their isomers from biological matrices. These include ion-pairing extraction,[29,30,65–67] methanol (MeOH) extraction,[47,68–70] acetonitrile (ACN) extraction,[44,62,71–74] and alkaline digestion followed by organic solvent extraction[39,60,75–81] (Table 1 and Fig. 2). Ion-pairing extraction uses a tetrabutylammonium hydrogen sulfate (TBAS) solution with a buffer to maintain pH during the extraction process. Anionic PFAS form ion pairs with the positively charged quaternary ammonium groups of TBAS. The resulting ion pairs exhibit enhanced solubility in organic solvents, such as methyl *tert*-butyl ether (MTBE), enabling efficient extraction of PFAS from biological samples. For biota with high lipid content, nonpolar solvents such as hexane are often used, followed by solid-phase extraction (SPE) using a silica gel column for further clean-up of the extract.[65] Often, alkaline digestion of tissue samples is performed to facilitate the breakdown of organic matter and release PFAS that may be bound within the biological matrix.[82,83] Following digestion, samples undergo organic solvent extraction using MeOH with an alkaline modifier. The most common alkaline modifiers are sodium hydroxide (NaOH) and potassium hydroxide (KOH). This is also the method described in EPA 1633A[48] for PFAS extraction from tissue samples. After evaporating the organic solvent, water was added prior to the SPE, where commonly used SPE cartridges in these methods include weak anion exchange (WAX),[31,39,41,60,67,68,73,78,84] mixed-mode C8

Table 1 Summary of the research papers on PFAS isomers reviewed in this paper from January 2000 to December 2025

Publication year[ref.] sample matrix	Sample extraction procedure	Instrument	Analytes	Major relevant findings
2004 [97] polar bear	Ion pairing extraction: TBAS solution (adjusted to pH 10) $Na_2CO_3/NaHCO_3$ buffer MTBE	GC-MS	PFOA	Seven PFOA isomers were separated, while others were total branched (T-Br) PFCAs and L-PFCAs
	Derivatized to 2,4-difluoroanilide analogues by 1,3-dicyclohexylcarbodiimide and 2,4-difluoroaniline		PFNA	Br-isomers were expressed relative to the L-PFCAs using peak areas
			PFDA	Greenland samples contained: Br-PFOA-5%, Br-PFNA-0.3%, Br-PFDA-1.4%, Br-PFUnDA-2.8%, Br-PFDoDA-2.1%, Br-PFTrDA-0.4%
			PFUnDA	Out of seven Br-PFOA, two isomers were observed
			PFDoA	Canadian samples only had L-PFOA, and others were Br-PFNA-0%, Br-PFDA-2.9%, Br-PFUnDA-1.2%, Br-PFDoDA-3.6%, Br-PFTrDA-ND
			PFTriDA	
2008 [29] lake trout	Ion pairing extraction: TBAS solution (adjusted to pH 10) $Na_2CO_3/NaHCO_3$ buffer	LC-MS/MS	PFOA	Study period: 1979–2004
			PFNA	Only L- and Br-isomers of PFUnDA and PFTriDA were observed
	MTBE		PFDA	Br-isomers were expressed relative to the L-PFCAs using peak areas
	MeOH		PFUnDA	Trends of the L- and Br-isomers of PFUnDA and PFTriDA were comparable in early samples, showing an increase from 1979 to 1983
	Filter – 0.2 μm nylon filters		PFDoA	By 1988, the Br-isomer trend deviated from the L, decreasing to only small amounts by 2004
			PFTriDA	
2008 [47] zooplankton, mysids, diporeira, alewife, smelt, sculpin, lake trout	MeOH extraction: MeOH	LC-MS/MS	PFOS	Br-PFOS concentrations were calculated using L-PFOS
	50% MeOH : water			Seven PFOS isomers were separated: L-PFOS, 3 mono-PFOS, and 3 di-PFOS
	Filter – 0.2 μm GHP filters			L-PFOS was dominant with 88–100% to T-PFOS, while di-PFOS was not observed
				PFOS isomer profiles in invertebrates resembled those in the sediment
				Mono-PFOS in all fish is in higher proportions than in invertebrates
				L-PFOS and mono-PFOS bioaccumulated in the Lake Ontario food web: positive BMFs and TMFs were observed
2008 [62] zooplankton, arctic cod, seal	ACN extraction: ACN	LC-MS/MS	PFOS	Relative peak areas were used
	ENVI-carb		PFHxA	Br-PFOS were ~50% in fish, 4% in seal
	Glacial acetic acid		PFHpA	L-PFOS biomagnifies more strongly through the food chain
			PFOA	Br-PFCAs were not detected
			PFNA	
			PFDA	
			PFUnDA	
			PFDoA	
2009 [65] clam, shrimp, oyster toadfish, snapper, catfish, atlantic croaker, kingfish, stingray, silver perch, spot, inshore lizardfish, tomtate, sea robin, black sea bass, large mouth bass, shark	Ion pairing extraction: TBAS solution (adjusted to pH 10)	LC-MS/MS	PFOS	T-Br-PFOS was considered

Table 1 *(Contd.)*

Publication year[ref.] sample matrix	Sample extraction procedure	Instrument	Analytes	Major relevant findings
	Na_2CO_3/$NaHCO_3$ buffer			L-PFOS is the most prevalent among PFAS, followed by Br-PFOS isomers
	MTBE			Statistically significant relationships with L-PFOS and Br-PFOS were shown
	MeOH Filter – 0.2 μm nylon filter For lipid rich samples, extraction followed with hexane Silica gel SPE 95% ACN in water MeOH			
2009 [90] bottlenose dolphins, ringed seals, alewife, rainbow smelt, sculpin, *Diporeia*, Mysis, lake trout	Ion pairing extraction: TBAS solution (adjusted to pH 10)	GC-MS	PFOA	Eight PFOA isomers were separated
	Na_2CO_3/$NaHCO_3$ buffer		PFNA	L-PFOA predominated (~90%), while L-PFNA, iso-, and di-PFNA were detected
	MTBE			In dolphins, PFOA isomers were detected in the order: P5CA < P3CA ≈ P3CA < P6CA < L
	Derivatized to 2,4-difluoroanilide analogues by 1,3-dicyclohexylcarbodiimide and 2,4-difluoroaniline			In dolphins, PFNA isomers were detected in the order: PFNA-1, L-PFNA, PFNA-3, PFNA-4, and iso-PFNA
2009 [91] rainbow trout	Ion pairing extraction: TBAS solution (adjusted to pH 10)	GC-MS	PFOA	Eight PFOA isomers were separated
	Na_2CO_3/$NaHCO_3$ buffer		PFNA	Enrichment of L-PFOA and L-PFNA over most Br-isomers was observed across all tissues
	MTBE			Heart and spleen were more enriched in L-isomers than the liver, blood, and kidney
	Derivatized to 2,4-difluoroanilide analogues by 1,3-dicyclohexylcarbodiimide and 2,4-difluoroaniline			PFOA-8 and L-PFOA displayed highest accumulation than other PFOA isomers and had highest half-life ($t_{1/2}$) L-PFNA had the longest $t_{1/2}$ followed by iso-PFNA
2009 [68] cromer crab, carp roe, spider crab	MeOH extraction + alkaline digestion: MeOH Aqueous KOH	LC-MS/MS	PFOS	Br-isomers were not quantified
	WAX SPE			Spider crabs have a majority of Br-PFOS while carp roe and cromer crab have a majority of L-PFOS
	Ammonium acetate 0.1% NH_4OH in MeOH MeOH			Br-PFOS were detected in most of the samples, carp roe and cromer crab showed a majority of L-PFOS
2009 [92] herring gull, double-crested cormorant (DCC), polar bear	Alkaline digestion: KOH in ACN/water	GC-MS	PFOS	Br-isomers were quantified
	WAX SPE			In Herring gull, DCC, and polar bear liver samples, L-PFOS accounted for >90% of T-PFOS
	1% NH_4OH in MeOH			All mono-PFOS isomers were detected in Herring gull eggs, DCC eggs, and polar bear
	MeOH In-port derivatization: TBAS in diethyl ether			Di-PFOS < LOD
2010 [66] zebrafish, rainbow trout	Ion pairing extraction: TBAS solution (adjusted to pH 10)	LC-MS/MS	PFOS	Eight PFOS isomers were analyzed
	Na_2CO_3/$NaHCO_3$ buffer			In zebrafish and trout parr, Br-PFOS isomers accumulated lesser than L-PFOS

Table 1 *(Contd.)*

Publication year[ref.] sample matrix	Sample extraction procedure	Instrument	Analytes	Major relevant findings
	MTBE			Elimination of Br-PFOS were more pronounced in the kidney and gill
	MeOH			The isomer profile in eggs showed no significant difference compared to that of adult fish: maternal transfer of Br- and L-PFOS isomers in fish are non-isomer specific
	Filter – 0.2 μm nylon filters			Isomer uptake pattern of Br-PFOS showed, P1 > di-2 > P6 > di-3 ~ P3 ~ P4 ~ P5 > di-1
				Maternal transfer pattern showed, L > mono > di-PFOS
2010 [98] herring gull	Alkaline digestion: KOH in ACN/water	GC-MS	PFOS	L-PFOS, 6 mono-PFOS, and 3 di-PFOS were analyzed and quantified
	WAX SPE			Eggs contained 95.0% and 98.3% L-PFOS
	1% NH_4OH in MeOH			All mono-PFOS isomers were detected, with the pattern P6 > P5 > P4 > P3
	MeOH			>60% of samples contained di-PFOS: P35 and P45 in Toronto Harbour, P35 in Chantry, and Fighting Island, P45 in Gull Island
	In-port derivatization: TBAS in diethyl ether			
2011 [75] fish, crab, mussel	Alkaline digestion: NaOH in MeOH	UPLC-MS/MS	PFHxS	Accumulation resulted in enrichment of L-PFOS (87–90%)
	ACN		PFHpS	Accumulated highest level isomers were P6 (3.8–7.1%) and P3, P4, P5 (2.5–4.1%)
	Hexane		PFOS	All PFOA isomers remained in the water body, showing no significant tissue accumulation
	ENVI-carb		PFDS	
	Glacial acetic acid		PFOA	
	Filter – 0.2 μm nylon filters		PFOSA	
2011 [71] grey seals	ACN extraction: ACN	LC-MS/MS	PFOS	Study period: 1974–2008
	ENVI-carb		PFOSA	Only L-isomers were quantified
	Glacial acetic acid		PFOA	Br-PFCAs were not observed
			PFNA	L-PFOS and L-PFOSA dominated in the samples
			PFDA	Br-PFOS isomers % increased over time, with a maximum in 2004
			PFUnDA	Sum of Br-PFOS isomers rose from 7% in 1974 to 22% in 2005
			PFDoA	Sum of Br-FOSA isomers increased from 2% in 1969 to 28% in 2004
			PFTriDA	
			PFTeDA	
2012 [72] zooplankton, lake trout, alewife, sculpin, round goby, rainbow smelt, mysid, *Diporeia*	ACN extraction: ACN	LC-MS/MS	PFOS	P1 enantiomers were analyzed
				Zooplankton had the first eluted enantiomer enriched, while *Diporeia* and mysids enriched with the second eluted enantiomer
				P1 was racemic in sediment, water, sculpin, and rainbow smelt
				P1 was nonracemic in the lake trout and in all invertebrate species
2012 [76] pilot whale, minke whale, fin whales, ringed seal, harbor porpoise, hooded seal, atlantic white-sided dolphin	Alkaline digestion: NaOH in MeOH	UPLC-MS/MS	PFOS	Study period – 1984–2009
	ACN		PFOA	Br-PFOA were not detected
	HCl in MeOH			Whale contained Br-PFOS: 6–7% compared to seal 9–17%

Table 1 *(Contd.)*

Publication year[ref.] sample matrix	Sample extraction procedure	Instrument	Analytes	Major relevant findings
	Hexane			In pilot whale, the PFOS isomer pattern remained relatively constant across sampling years
	ENVI-carb			In ringed seals, there was a decrease in L-PFOS over time: 91% in 1984 → 83% in 2006
	Glacial acetic acid Filter – 0.2 μm GHP filters			
2013 [42] polar bear	Alkaline digestion: KOH in ACN/water	LC-MS/MS	PFOS	PFOS isomers were analyzed: L-PFOS, 6 mono-PFOS (P1, P2, P3, P4, P5, P6), 4 di-PFOS (P55, P44, P45, P35)
	WAX SPE	GC-MS		L-PFOS accounted for 93.0% in the liver and lower in blood 85.4%
	1% NH_4OH in MeOH			Mono-PFOS were detected in blood and liver, but not in brain, muscle, and adipose
	MeOH In-port derivatization: TBAS in diethyl ether			Di-PFOS were not detected L-PFOS and P1 were enriched in tissues In both liver and blood, P6 was identified as the dominant Br-isomer (2.61% and 3.26%)
2014 [41] fish, shellfish	Hexane 3 : 1 tetrahydrofuran (THF)/water Water	UPLC-MS/MS	PFOS PFOA	Method validation study Isomers were not quantified Br-PFOS isomers were detected in nearly all fish and shellfish samples where Br-PFOA were not detected
	WAX SPE Acetate buffer 1 : 1 THF/ACN mixture ENVI-carb cartridge 0.1% NH_4OH in MeOH Graphitized carbon cartridge Filter – 0.2 μm cellulose filters			
2014 [77] lake trout	Alkaline digestion: NaOH in 1 : 1 MeOH : ACN	UPLC-QToF/MS	PFHpS	Method validation study
	MeOH ENVI-carb		PFOS PFDS	Isomers were not quantified In trout, L-PFOS was present at higher levels than Br-PFOS compared to the standard
	Glacial acetic acid		PFOA PFUnDA	Presence of Br-PFHpS, Br-PFDS and Br-PFUnDA observed
2014 [67] shrimp, *Pelteobagrus fulvidraco*, minnow, lake saury, carp, mongolian culter, mud fish, gobies	Ion pairing extraction: TBAS solution (adjusted to pH 10)	UPLC-MS/MS	PFOS	L-PFOS was the predominant PFOS isomer in most tissues, ranging from 46.3–96.5%
	Na_2CO_3/$NaHCO_3$ buffer		PFOA	In eggs compared to liver, PFOS isomers followed the order: L- > mono- > di-isomers
	MTBE			Liver/muscle and kidney/muscle ratios of L-PFOS were higher than those of Br-isomers
	MeOH			L-PFOA was the dominant isomer across all tissues and eggs
	Carbon SPE			Proportions observed: muscle: 91.9–100%, kidney: 94.5–98.6%, liver: 93.8–100% (except 35.5% in mud fish liver), eggs: 72.9–100%, head: 100%
	MeOH Water WAX SPE Ammonium acetate buffer MeOH 0.1% NH_4OH/methanol Filter – 0.2 μm nylon filters			

Table 1 *(Contd.)*

Publication year[ref.] sample matrix	Sample extraction procedure	Instrument	Analytes	Major relevant findings
2014 [31] Japanese medaka	MeOH extraction: MeOH	GC-MS & UPLC-MS/MS	PFOS	Seven Br-PFOS isomers were separated
	Water		diSPAP	Biotransformation pathways from diSPAP to PFOS in medaka were proposed, including isomer-specific biotransformation
	WAX SPE		PFOSA	Br-isomers for all target chemicals except for NEtFOSA and NEtFOSE were detected
	0.5% NH_4OH in MeOH		FOSAA	Br-isomers of diSPAP were preferentially enriched in medaka exposed to diSPAP
	In-port derivatization, TBAS in diethyl ether		NEtFOSA	Metabolism of Br-isomers preferred leading enrichment of Br-PFOS
			NEtFOSAA	Enrichment of B-PFOS was greater
			NEtFOSE	for P3, P4, and P5
2014 [44] herring	ACN extraction: ACN	UPLC-MS/MS	PFOS	Study period: 1991–2011
	Water		PFOSA	L- and T-Br-isomers have studied
	Mixed mode C8 + aminopropyl SPE			PFOS and FOSA had <10% Br-isomers to T-PFOS and T-PFOSA
	2% formic acid			L-PFOS did not change significantly over the study period
	Water			Br-PFOS decreased over the time: 1991 and 2011 from 7% to <4%
	MeOH			Br-PFOSA levels decreased: 1991 and 2011 from 10% to <3%, and L-PFOSA increased
	2% NH_4OH in MeOH			
2015 [30] common carp	Ion pairing extraction: TBAS solution (adjusted to pH 10)	LC-MS/MS	PFOS	*In vivo* tests, Br-PFOSA and Br-PFOS were eliminated faster, thereby enriching L-PFOSA
	Na_2CO_3/$NaHCO_3$ buffer		PFOSA	Six PFOS isomers were detected
	MTBE			Elimination order: L-PFOS < P2 < L-PFOSA ≈ P6< P3,P5 < P4 < P1 < Br-PFOSA
	MeOH			Br-PFOS were enriched in fish, indicating the preferential metabolism of Br-PFOSA isomers to Br-PFOS
	Filter – 0.2 μm nylon filters			The abundance of Br-PFOS followed the order liver > blood ≈ kidney > muscle
2015 [99] European chubs, common breams, crucian carp, common carp, nase carp	ACN extraction: water	UPLC-MS/MS	PFOS	Both Br- and L-PFOS were detected where L-PFOS was found in high abundance
	Formic acid		PFOSA	
	ACN			
	Anhydrous $MgSO_4$			
	Sodium chloride			
	C18 silica sorbent			
	MeOH			
	Filter – 0.2 μm nylon filters			
2015 [73] invertebrates: mollusk, short-necked clam, rock shell, Chinese mitten-handed crab	ACN extraction: ACN	GC-MS	PFOA	Five PFOA isomers were separated (L-PFOA, P3CA, P4CA, P5CA, P6CA)
Fish: red-eye mullet, small yellow croaker, Japanese mackerel, Spanish mackerel, half-smooth tongue-sole, flathead fish, black spot-fed bass, China anchovy	Water		PFNA	L-PFOA, P6CA, L-PFNA, L-PFDA, iso-PFDA, L-PFUnDA, iso-PFUnDA, L-PFDoDA, iso-PFDoDA, L-PFTriDA, iso-PFTriDA and L-PFTeDA and iso-PFTeDA were detected
	WAX SPE		PFDA	P6CA is the only Br-PFOA detected in marine samples
	0.5% NH_4OH in MeOH		PFUnDA	L-PFCAs showed significant positive relationships with trophic levels
	Activated charcoal cartridges		PFDoDA	Br-PFCA isomers' correlations were positive but not statistically significant

Table 1 *(Contd.)*

Publication year[ref.] sample matrix	Sample extraction procedure	Instrument	Analytes	Major relevant findings
	In-port derivatization: TBAS in diethyl ether		PFTriDA	
			PFTeDA	
2016 [100] common carp	Ion pairing extraction: TBAS solution (adjusted to pH 10)	UPLC-MS/MS	PFOS	L-PFOS was preferentially accumulated compared with Br-isomers
	Na_2CO_3/$NaHCO_3$ buffer			Among Br-isomers: P1 showed the highest bioaccumulation, P2 showed the lowest bioaccumulation
	MTBE			L-PFOS demonstrated greater partitioning ability from blood to other tissues compared with Br-PFOS
	MeOH			L-PFOS had the greatest uptake following P1 > P4 > P3, P5 > P2
	Filter – 0.2 μm nylon filters			Elimination order: P2 > P4> P3, P5 ≈ P6 > L > P1
				Br-PFOS isomers were more preferentially eliminated from the kidney or gill than L-PFOS
2016 [87] ringed seal, polar bear, killer whale	ACN extraction: ACN	UPLC-MS/MS	PFOS	Isomer patterns differed in whales compared to ringed seals and polar bears
	WAX SPE		PFOSA	L-PFOS: polar bears: 88.4%, killer whales: 89.8%, ringed seals: 92.1%
	MeOH			L-PFOSA proportions: polar bears: 98.5%, killer whales: 94.4%, ringed seals: 95.0%
	1% NH_4OH in MeOH			PFOSA/PFOS ratios of Br-isomers, L-isomer, and T-isomers in ringed seals and polar bears were not significantly different
	Filter – 0.2 μm nylon filters			Killer whales' isomer ratios were significantly higher
2016 [84] zooplankton, herring, sprat, guillemot	ACN extraction: ACN	UPLC-MS/MS	PFOS	L- and T-Br-isomers were analyzed
	Water		PFOSA	L-PFOSA (33%-55%), L-PFOS (74%-88%), and Br-isomers were detected in all samples
	WAX SPE			L-PFOS was significantly abundant compared to L-PFOSA and their branched counterparts
	MeOH			With the increase of trophic level, percentage L-PFOSA had a significant decline trend
	1% NH_4OH in MeOH			L-PFOS observed between sprat and zooplankton, between sprat and guillemot eggs were significantly different
	Filter – 0.2 μm nylon filters			L-PFOSA was significantly lesser in guillemot eggs compared to sprat
2016 [101] crucian, flounder, carp, hairtail, yellow croaker, weever, silver carp	Ion pairing extraction: TBAS solution (adjusted to pH 10)	LC-MS/MS	PFOS	Fish contained PFOA isomers: L-PFOA, P4CA, P5CA and P6CA isomers and PFOS isomers: L-PFOS, P1, P2, P3, P4, P6
	Na_2CO_3/$NaHCO_3$ buffer		PFOA	L-PFOS was enriched, with proportions of 84.8% in fish while L-PFOA with proportions of 92.2%
	MTBE			In the order: P4CA > P6CA > P5CA were detected
	MeOH			In the order: P3, P5 > P6 > P4 > P1 > P2 were detected
	Carbon (Pesti-carb) SPE MeOH			
	Filter – 0.2 μm nylon filters			
2017 [102] south polar skua, snow petrel, king penguin	ACN extraction: ACN	LC-MS/MS	PFOS	Only L-PFOS was reported in all the samples

Table 1 *(Contd.)*

Publication year[ref.] sample matrix	Sample extraction procedure	Instrument	Analytes	Major relevant findings
	Water on-line SPE			
2018 [78] crucian carp	Alkaline digestion: KOH in MeOH	LC-MS/MS	PFOS	Br-PFOA (P3CA, P4CA, P5CA, and P6CA), PFOS (P1, P3/P4, P5, and P6,) and T-Br-PFOSA were reported
	Ion pairing extraction: TBAS solution (adjusted to pH 10)		PFOA	Br-PFOSA and all Br-isomers of PFOA and PFOS were found in detectable concentrations
	Na_2CO_3/$NaHCO_3$ buffer			All Br-PFOA, L-PFOS, and L-PFOSA were detected in >80% of the samples from all tissues
	MTBE			Tissue/blood ratio in bile were isomer-specific with all Br-PFOA and Br-PFOS (except P1) being more efficiently transferred to bile compared to the L-isomers
	Water			Br-PFOS and Br-PFOA had consistently lower bioaccumulation compared to the L-isomers
	WAX SPE			
	MeOH			
	0.1% NH_4OH in MeOH			
2019 [79] invertebrates: waterlouse, water boatmen, freshwater amphipods, roundworm, mayflies, caddisflies, damselflies/ dragonflies	Alkaline digestion: NaOH in MeOH	UPLC-MS/MS	PFPeS	The Br-PFOA were identified from 0.0–6.6%, 0.0–18% for Br-PFHpS and 15–28% for Br-PFOS
	Water		PFHxS	Br-PFOS bioaccumulated lower compared to L-PFOS, while lowest being di-PFOS and similar values for P3/P4/P5, P6/P2 and P1
	ENVI-carb		PFHpS	
	Glacial acetic acid		PFOS	
	Water		PFOA	
	WAX SPE			
	MeOH			
	0.1% NH_4OH in MeOH			
2019 [103] carp	Ion pairing extraction: TBAS solution (adjusted to pH 10)	LC-MS/MS	PFHxS	L-PFOS was eliminated more *via* feces
	Na_2CO_3/$NaHCO_3$ buffer		PFOS	L-PFHxS was eliminated more *via* urine
	MTBE			L-isomers were preferentially accumulated in fish compared to Br-isomers
	MeOH			L-PFOS in the blood was higher than that in the liver and kidney
	Filter – 0.2 μm nylon filters			
2020 [80] eastern oyster	Alkaline digestion: KOH in MeOH	LC-MS/MS	PFOS	L-PFOS, T-mono-PFOS and T-di-PFOS were analyzed
	ENVI-carb			Both L- and Br-PFOS were detected in exposed samples
				L-PFOS remained at high levels in samples during depuration while Br-isomer was almost eliminated from the tissue
2020 [81] blue spot gobies	Alkaline digestion: NaOH in MeOH	LC-MS/MS	PFOS	L- and Br-PFOS were analyzed and detected
	Acetic acid			Depuration rates L-PFOS > L + Br-PFOS with $t_{1/2}$ of 15, and 16 d, respectively
	Primary secondary amine & C18			Enrichment of L-PFOS (70–90%) throughout the depuration period was observed
	Filter – 0.45 μm polyethersulfone filters			

Table 1 *(Contd.)*

Publication year[ref.] sample matrix	Sample extraction procedure	Instrument	Analytes	Major relevant findings
2020 [104] invertibrates: aquatic insect larvae (elongated-flies, mayflies, alderflies, damselflies, dragonflies, caddisflies, crayfish, amphipods, water louses, back-swimmers, aquatic spiders, roundworms, diving beetle, aquatic beetles, freshwater snails)	Alkaline digestion: NaOH in MeOH	UPLC-MS/MS	PFHxS	Contained significantly low Br-isomers: Br-PFOS < 18%, Br-PFHxS < 8%
	MeOH Water		PFOS	L-isomers were enriched BMF of Br-PFHxS were lower compared to L-PFHxS with 4/2-PFHxS being the lowest
	WAX SPE			BMF for Br-PFOS were up to 1 magnitude lower and significantly different to L-PFOS
	0.1% NH_4OH in MeOH Filter – 0.2 μm GHP filters			
2020 [105] fish (from the market)	Alkaline digestion NaOH in methanol	LC-MS/MS	PFOS	Method validation study Five mono- and 1 di-PFOS were quantified and reported as sum
	ACN			L and Br-PFOS isomers were detected in the samples
	Acetic acid Water WAX SPE MeOH			
2021 [70] zooplankton, crabs, sculpin, wolffish, glaucous gull	MeOH extraction: MeOH	LC-MS/MS	PFOS	L-PFOS and T-Br-PFOS were analyzed
	ENVI-carb			PFOS isomer profile was enriched by the L-PFOS (78%–91%)
	Filter – 0.2 μm microcentrifuge filter			Benthic organisms showed PFOS isomer patterns similar to sediment L-PFOS enrichment was greater in benthic organisms compared to pelagic organisms
2021 [69] double-spotted queenfish, marbled spinefoot, bigeye scad, strongspine silver-biddy, bluefin trevally, bonefish	MeOH extraction: MeOH	LC-MS/MS	PFOS	L-PFOS and T-Br-PFOS were analyzed
	ENVI-carb			L-PFOS was abundant in fish liver and muscles: 96.4% and 90% of T-PFOS respectively
	Filter – 0.2 μm microcentrifuge filter			Low Br-PFOS% observed in the high trophic double spotted queenfish (25.0%) fish compared to the bigeye scad (37.3%)
2021 [86] aquatic insect larvae, emergent aquatic insects	Alkaline digestion: NaOH in MeOH	LC-MS/MS	PFHxS	Br-PFOS isomers were consistently detected at lower proportions (0–20%)
	MeOH		PFOS	Br-PFHxS isomers were not discussed
	Water ENVI-carb cartridges WAX SPE 0.1% NH_4OH in MeOH			
2021 [74] bivalve: mangrove cupped oyster, mangrove shellfish, clam, mangrove oyster, stout tagelus, polychaeta, fish: mullet, torroto grunt, mojarra, silverjenny, mada-mango sea catfish, fat snook, drum, trevally, catfish, common snook, barbel drum, crustacean: blue crab, ucides, whiteleg, shrimp, mangrove tree crab	Alkaline digestion: ACN	UPLC-MS/MS	PFHxS	The L and Br-isomers of pre-PFOS: PFOSA and EtFOSA were detected in biota
	NaOH in ACN		PFOS	TMFs > 1 were observed for L- and Br-PFOS, L- and Br-EtFOSA

Table 1 *(Contd.)*

Publication year[ref.] sample matrix	Sample extraction procedure	Instrument	Analytes	Major relevant findings
	Water Formic acid Ammonium formate		PFOA EtFOSA	
2021 [106] marine and freshwater fish	Alkaline digestion: NaOH in MeOH	UPLC-MS/MS	PFOS	Eight Br-isomers for PFOS and PFOA were analyzed
	Water WAX SPE NH_4OH in MeOH		PFOA	L-PFAS were abundant Br-PFOS in freshwater fish was higher than that in marine fish L-PFOS accounted for in freshwater fish: 42.8% and marine fish: 34.3% of T-PFAS The detection frequencies of P3/P4, P5 and P6 (40–60%) were higher in freshwater fish than in marine fish (9%) L-PFOA was 2.2% and 0.9% of T-PFAS in freshwater and marine fish, respectively No Br-PFOA were found
2022 [107] common carp	Ion pairing extraction: TBAS solution (adjusted to pH 10) $Na_2CO_3/NaHCO_3$ buffer	UPLC-MS/MS	PFOS PFOSA	L-, 1m-, 3 + 4 + 5m-, iso-PFOSA were separated Compared to the exposure PFOSA solution, L-PFOSA was slightly enriched in the fish with 77.9%, while 3 + 4 + 5m-, iso-, and 1m-PFOSA were lower (0.2–12.1%)
	MTBE MeOH Carbon (Pesti carb) SPE Methanol			BCFs of PFOSA isomers followed the order: 1m-<3 + 4 + 5m- ≈ 6m < L BCFs of PFOS isomers followed the order: P6 < P3 + P4 + P5 ≈ L < P1 P1 had higher % (5.5%) than in the exposure solution (3.4%) BTAFs of PFOS isomers (from PFOSA biotransformation) followed the order: P < L < P6 ≈ P3 + P4 + P5
2023 [45] shrimp, crab, fish, finless porpoises, Indo-Pacific hump-back dolphins	Alkaline digestion: NaOH in ACN	UPLC-MS/MS	PFOS	*cis*- and *trans*-PFECHS isomers were reported
	HCL ENVI-carb SPE ACN Water WAX SPE 0.1% NH_4OH in MeOH		PFECHS	TMFs of *cis*-isomer: 1.92 and *trans*-isomer: 2.25 L-PFOS proportions to T-PFOS isomers were >85% Br-PFOA were only detected in the cetacean liver samples, accounting for <1% of T-PFOA TMF PFOS isomers: L > P6 > P5 > P4 > P3 No significant correlation was found between the two PFECHS isomer ratios in the marine food web
2024 [60] shark	Alkaline digestion: modified EPA 1633, KOH in MeOH ACN Water WAX SPE 1% NH_4OH in MeOH	LC-MS/MS	PFOS	L- and Br-PFOS were analyzed and detected in all the samples %L-PFOS was 79% in Caribbean reef sharks and 93% in the New York Bight sharks
2024 [61] sunfish, white perch, yellow perch, catfish	MeOH extraction: MeOH Dispersive carbon SPE Filter – 0.2 μm nylon filters	UPLC-dIMS-QToF/MS	PFHxS PFOS PFNS PFDS PFUdS PFDoS	Br-isomers of PFOS, PFHxS, PFNS, PFDS, PFUdS, and PFDoS were detected in every sample Only detection frequencies reported

Table 1 *(Contd.)*

Publication year[ref.] sample matrix	Sample extraction procedure	Instrument	Analytes	Major relevant findings
2024 [85] herring, cod, eelpout, guillemot gull	ACN extraction: ACN	UPLC-MS/MS	PFOS	Study period: 1980–2003
	Water		PFOSA	L-PFOSA concentrations were high in Kattegat herring (96%) compared to the Baltic Sea herring (63–74%)
	Mixed mode C8 + aminopropyl SPE			L-PFOS isomer fractions showed geographical variability: Bothnian Bay: similar to Kattegat (95%), Northern & Southern Baltic Proper: lower (77–89%)
	2% formic acid Water MeOH 2% NH_4OH in MeOH			
2024 [108] king penguin	ACN extraction: ACN Water on-line SPE	LC-MS/MS	PFOS	Br-PFOS were not detected L-PFOS was the dominant in both types of fast (molting: 2.64–5.96 ng g^{-1}; breeding: 3.5–7.5 ng g^{-1}) L-PFOS concentrations increased in plasma during both types of fasting, molting, and breeding L-PFOS change during the molting fast did not indicate excretion into feathers
2025 [43] Crucian carp	ACN extraction: ACN	LC-MS/MS	PFPeSF	Br-isomers contributing 16–25% of T-PFASF
	Chemical derivatization: *p*-toluenethiol in ACN		PFHxSF	In fish samples, Br-PFPeSF (16%), Br-PFHxSF (25%), Br-PFHpSF (17%), and Br-PFOSF (21%) were detected compared to their L-isomers
	Triethylamine in ACNACN		PFHpSF	log BAF of L-PFASF increased from 1.7 (l-PFBSF) to 3.0 ± 0.27 (l-PFOSF) with the increase of carbon chain length
			PFOSF	L-PFASFs were preferentially bioaccumulated Br-isomers of detected PFASF displayed lower log BAF values than their respective L-isomers
	Water		PFOA	L-PFOA (0.52 ng g^{-1}) detected higher than L-PFOS (0.32 ng g^{-1})
	WAX SPE			Br-PFOA followed the order of concentrations: P6CA > P4CA ≈ P5CA while Br-PFOS followed the order: P6 > P5 P3/P4 > P1
	NH_4OH in MeOH			
2025 [95] alligator	ACN extraction: ACN	UPLC-dIMS-QToF/MS	PFUnDA	Novel Br-PFUnDA was identified for the first time
	40 : 60 MeOH : water		Unsaturated PFOS	Two new isomers of Nafion Byproduct 2 (NB2) were detected
	Ammonium acetate		NB2	Across samples, the L-isomer dominated (94% by concentration)
2025 [109] clam	QueChERS	LC-MS/MS	PFOA	Samples contained 94% L-isomer (~18 ng g^{-1}) by concentration
	Water, ACN, formic acid $MgSO_4$, NaCl dSPE Water Strata-XL-AW SPE NH_4OH in MeOH Filter – 0.2 μm nylon filters			
2025 [39] blue catfish, cod, haddock, rainbow trout, coho salmon, atlantic salmon, tilapia (from the market)	Alkaline digestion: modified EPA 1633A, KOH in MeOH	UPLC-cIMS-QToF/MS	PFOS	L-PFOS, mono-PFOS: P1–P6 and di-PFOS: P35, P45, P55 were separated and quantified

Table 1 *(Contd.)*

Publication year[ref.] sample matrix	Sample extraction procedure	Instrument	Analytes	Major relevant findings
	ACN		PFOA	L-PFOA and mono-PFOA were separated and analyzed
	Water			L-PFOS in all the fish samples was only 27–40% of the T-PFOS concentration
	GCB/WAX SPE			Cod had highest L-PFOS (0.670 ng g^{-1}), while tilapia had the lowest (0.30 ng g^{-1})
	NH_4OH in MeOH & ACN			L-PFOA was ~99% of T-PFOA which is higher than the standard
	Cold MeOH clean up			Habitat-specific PFOS isomer patterns were observed
	Ammonium acetate			Benthic fish contained L-PFOS and all mono-isomers
				Pelagic fish contained L-PFOS but fewer monosubstituted types
2025 [110] black-browed albatrosses, white chinned petrels, common diving petrels	ACN extraction: ACN	UPLC-MS/MS	PFOS	Br-PFOS proportions were greater in 2014 compared to 2004 in white-chinned petrels and common diving petrels
	ENVI-carb			Indicated temporal variability in PFOS isomer profiles, with Br-PFOS increasing over time in seabird tissues
	Acetic acid Ammonium acetate			
2025 [40] double-crested cormorant	ACN extraction: ACN	UPLC-cIMS-QToF/MS	PFOS	L-PFOS, mono-PFOS: P1–P6 and di-PFOS: P35, P45, P55 were separated and quantified
	Carbopack™ GCB with ACN			All Br-PFOS had higher ionization efficiencies (more than 2 to 5 times higher) than L-PFOS
	Ammonium acetate			Detected PFOS isomers showed the distribution: L-PFOS: 88.5%, P3/P4/P5: 4.3%, P6: 3.1%, P1: 3.0%, P35/P45/P55: 1.2%
				Br-PFOS isomers were dominated in wastewater (more than 50% of total PFOS), while Br-PFOS is significantly declined in egg yolk samples (<12%)

The table includes details on which country conducted the study with the references, year, sample type, extraction methodology, analytical instrumentation, PFAS investigated, and a summary of the major findings relevant to isomer behavior or distribution. Perfluoroalkyl carboxylic acids (PFCAs), methanol (MeOH), acetonitrile (ACN), tetra-*n*-butyl ammonium hydrogen sulfate (TBAS), weak anion exchange (WAX) solid phase extraction (SPE), graphatized carbon black (GCB), ENVI-Carb and Carbopack™ are versions of graphitized carbon. Potassium hydroxide (KOH), sodium hydroxide (NaOH), magnesium sulfate ($MgSO_4$), ammonium hydroxide (NH_4OH), hydrochloric acid (HCL), liquid chromatography (LC), ultra-high performance LC (UPLC), gas chromatography (GC), mass spectrometry (MS), tandem mass spectrometry (MS/MS), quadrupole time-of-flight (QToF), drift tube ion mobility separation (dIMS), cyclic ion mobility separation (cIMS). United Kingdom (UK), United states (US), not detected (ND), biomagnification factor (BMF), trophic magnification factor (TMF), bioconcentration factor (BCF), total branched (T-Br), precursor PFOS (Pre-PFOS).

with aminopropyl (MAP),[44,85] and primary secondary amine combined with C18 (PSAC).[81] Elution is typically carried out using ammonium hydroxide (NH_4OH) in methanol, which enhances PFAS recovery by disrupting electrostatic interactions between the analytes and the sorbent.[65] During these solid–liquid extractions, some methods have used ENVI-Carb (graphitized carbon; dispersive SPE),[62,69,71,76,77,79] Sorbents such as graphitized carbon,[41,45,86] activated charcoal,[73] and WAX cartridges with graphitized carbon black (GCB) add-on (GCB-WAX)[39] have been used to improve the removal of lipids, proteins, and pigments that contribute significantly to the matrix effects during analysis of biota.[48]

Ion-pairing extraction is well-suited for blood and other liquid biological matrices because the addition of TBAS creates a hydrophobic ion-pair that enhances the partitioning of PFAS into nonpolar solvents such as MTBE. This effective phase transfer makes the technique particularly advantageous for isolating PFAS from complex liquid samples. In contrast, EPA Method 1633A[48] employs alkaline digestion, which is more appropriate for tissue matrices because it facilitates the liberation of strongly bound PFAS from solid biological material. A known limitation of the standard 1633A workflow is the manual addition of graphitized carbon black (GCB) during cleanup, a step that may introduce variability and

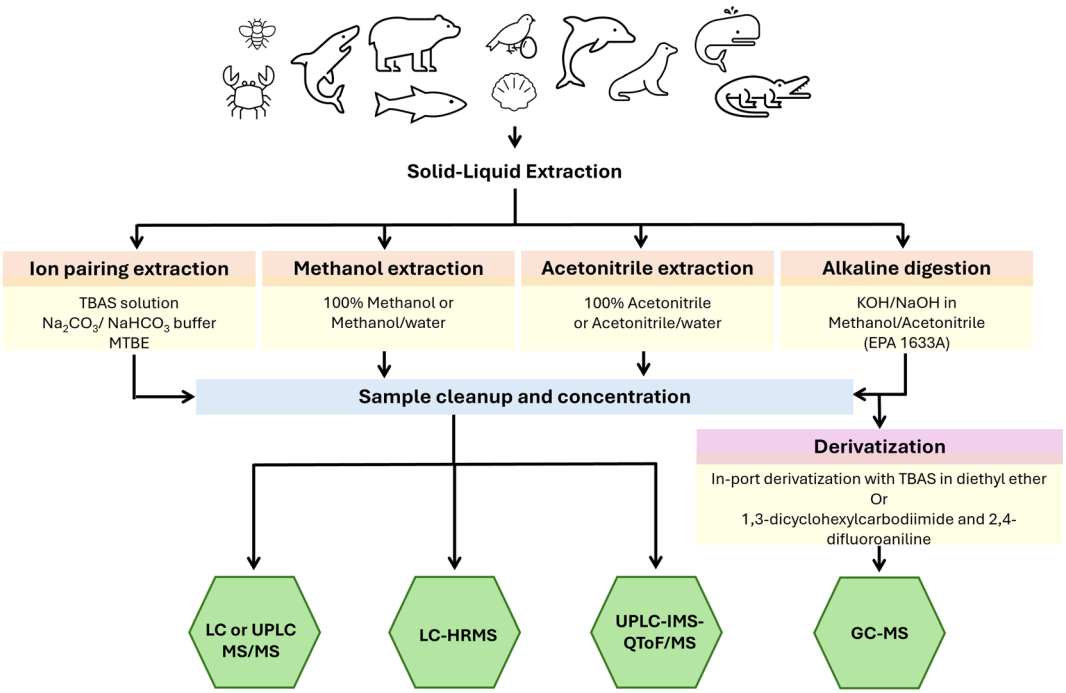

Fig. 2 Schematic diagram of extraction methods and instrumentation in fish analysis used from 2005–mid 2025. Abbreviations used: TBAS – tetrabutylammonium hydrogen sulfate, Na_2CO_3 – sodium carbonate, $NaHCO_3$ – sodium bicarbonate, KOH – potassium hydroxide, NaOH – sodium hydroxide, LC – liquid chromatography MS/MS – tandem mass spectrometry, UPLC – ultra-high-performance LC, HRMS – high resolution mass spectrometry, IMS – ion mobility separation, QToF/MS – quadrupole time-of-flight mass spectrometry, GC-MS – gas chromatography mass spectrometry.

reduce method reproducibility. However, a recent study[39] demonstrated that replacing manually added GCB with prepacked GCB-WAX SPE cartridges provides more consistent cleanup performance while also reducing labor and analysis time. Taken together, these findings highlight that ion-pairing extraction and alkaline digestion coupled with GCB-WAX SPE (representing a modified EPA Method 1633A) each offer distinct advantages, and the choice between them should be guided by the characteristics of the biological matrix under investigation.

4. Separation and detection of isomers

Analysis of non-volatile PFAS has primarily been performed using LC coupled with a tandem mass spectrometry (MS/MS) technique (Table 1 and Fig. 2). Using multiple reaction monitoring (MRM), some PFAS isomers can be identified and quantified based on differences in their fragmentation patterns and the intensities of diagnostic ions.[87] Although PFAS isomers often generate the same precursor ion, their structural differences cause them to fragment along different pathways. For example, L-isomers may produce a distinct pattern of product ions and different relative abundances compared to their Br-isomers. By monitoring multiple product ions from the same precursor and comparing their characteristic transition ratios, analysts can obtain unique mass-spectral "fingerprints" that enable reliable differentiation of individual isomers. For chromatographic separation of isomers, a variety of analytical columns have been employed, including longer C18 columns (100 mm to 150 mm),[29,62,75,88,89] pentafluorophenyl phase (PFP) columns,[47] and FluoroSep RP Octyl columns.[66] Longer C18 columns (100–150 mm) improved resolution compared to shorter formats but still yielded only partial separation of branched PFOS isomers. PFP columns and FluoroSep™ RP Octyl columns offered greater selectivity through π–π and fluorophilic interactions, enabling better distinction of L- and Br-PFOS. In one study, chemical derivatization was utilized to enable the analysis of sulfonyl fluoride compounds, which are precursor PFAS in LC-MS/MS. Unlike perfluoroalkyl sulfonates (PFSAs), sulfonyl fluorides are less stable and do not ionize efficiently in LC-MS/MS. The derivatization was carried out using *p*-toluenethiol and triethylamine in ACN, which allows the conversion of the sulfonyl fluoride group into a more stable thiol-derived product that ionizes readily, producing stronger and more reliable signals for quantification.[43]

While LC-MS/MS is the primary method for PFAS analysis, some studies have used gas chromatography mass spectrometry (GC-MS)[31,90,91] as shown in Table 1. For PFAS that are not inherently GC-amenable due to their low volatility and thermal instability, chemical derivatization is required for analysis. In some studies, in-port derivatization of PFAS was performed using tetrabutylammonium sulfate (TBAS) in diethyl

ether.[31,73] Conventional LC-MS/MS extraction methods often leave behind lipids and other interfering compounds that obscure signals, but the combination of WAX SPE and in-port derivatization significantly reduces this background noise. Through pyrolytic alkylation with TBAH, PFOS isomers are transformed into more volatile tertiary amine and butyl derivatives, making them amenable to analysis by GC-MS.[92] Alternatively, PFAS can be derivatized to their 2,4-difluoroanilide analogues by reacting with 1,3-dicyclohexylcarbodiimide and 2,4-difluoroaniline.[90,91]

One of the most recent and advanced analytical techniques for separating PFAS isomers is ion mobility spectrometry (IMS) coupled with LC-high-resolution mass spectrometry (LC-HRMS). IMS enables gas-phase isomer separation without derivatization by extending the ion's path length prior to mass analysis. This additional separation dimension allows for differentiation based on the ions' size, shape, and charge. Several IMS configurations are now used for PFAS analysis, including cyclic ion mobility spectrometry (cIMS)[39] that uses a cyclic ion path, and drift tube ion mobility spectrometry (dIMS)[61] that separates ions along a linear drift region. The separation of PFOS and PFOA isomers in a commercially available standard and a fish sample (benthic fish, haddock) utilizing cIMS is shown in Fig. 3, which is adopted from our recent publication.[39] Furthermore, a recent study reported the optimization of cIMS for distinguishing PFOS isomers,[40] with application to seabird eggs; a detailed discussion on this work is provided below. The addition of IMS provides the capability to resolve target analytes from coeluting matrix interferences and to separate structural isomers based on their distinct collision cross-section (CCS) values.[93]

While GC-MS has demonstrated strong capability for separating PFOS isomers, it requires additional sample preparation, including TBAH-based in-port derivatization in diethyl ether, which increases method complexity and introduces potential sources of variability. Despite this, GC-MS remains a valuable tool for identifying PFAS isomers following derivatization. Conventional LC methods, by contrast, often require columns with chiral stationary phases to achieve effective isomer separation and still frequently fail to fully resolve individual isomers. The cIMS overcomes these limitations by enabling isomer separation without derivatization or without the use of

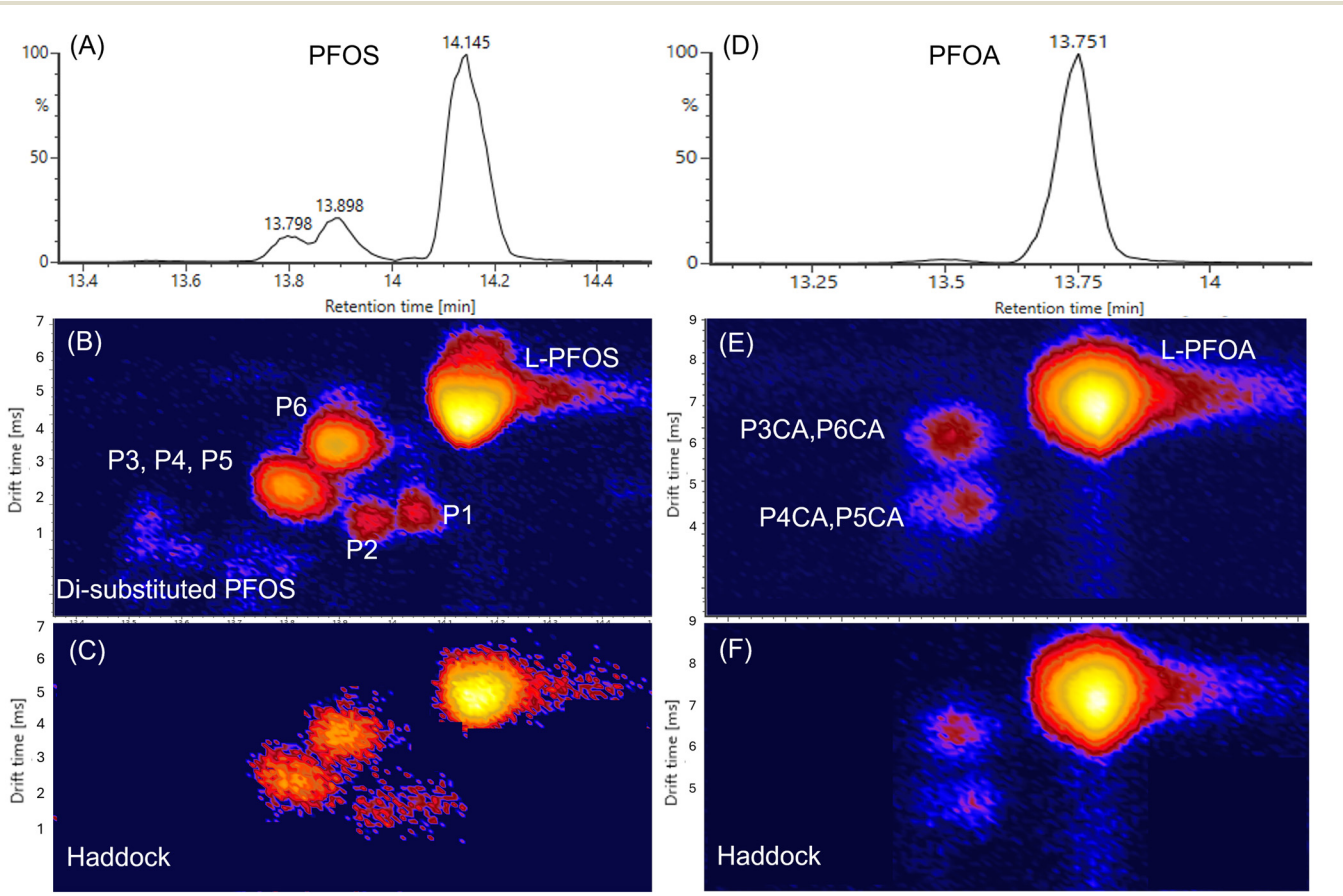

Fig. 3 cIMS separation of PFOS (6 passes) and PFOA (3 passes). (A) Chromatogram of a PFOS standard (50 ng g^{-1}); (B) mobilogram of the PFOS standard showing linear (L-PFOS), mono-substituted (P1–P6), and di-substituted PFOS isomers (P3, P4, and P5 co-eluting under current conditions); (C) mobilogram of PFOS isomers in haddock; (D) chromatogram of a PFOA standard (50 ng g^{-1}); (E) mobilogram of the PFOA standard showing linear (L-PFOA) and mono-substituted isomers (P3CA/P6CA and P4CA/P5CA co-eluting under current conditions); (F) mobilogram of PFOA isomers in haddock. Names of each isomer in this figure can be found in Fig. 4.

chiral LC columns, operating effectively with a standard C18 column. The added IMS dimensions of DT and CCS measurements substantially enhance structural discrimination and isomer identification. Recent studies have successfully applied cIMS to separate PFOS[39,40] and PFOA isomers[39] and to identify novel isomers produced through microbial degradation.[32] Although cIMS instrumentation is costly, integrating IMS capabilities provides significant advantages for isomer-specific analysis[94] and broader non-target workflows.[95]

5. Identification/nomenclature and quantification

In the absence of analytical standards, early studies assigned isomer names based on chromatographic elution order. For example, PFOA isomers were labeled PFOA-1 through PFOA-8, with L-PFOA corresponding to PFOA-2 and iso-PFOA (P6CA) designated as PFOA-5.[91] Similarly, PFNA isomers were named PFNA-1 to PFNA-4, where L-PFNA was identified as PFNA-2 according to their elution order in the chromatograph.[90] For PFOS isomers lacking individual standards, such as di-substituted PFOS (P35, P45, and P55), whose identities were unknown, researchers used the abbreviations DM1, DM2, and DM3, ordered by decreasing retention time.[66] In recent years, with the availability of standards for individual isomers,[40] the specific isomers for PFOS, PFOA, and PFOSA have been named accordingly, as in Fig. 4. In this review, the following abbreviations were adopted for clarity: linear as L-, branched as Br-, monomethyl-substituted as mono-, and dimethyl-substituted as di-. The term "iso" refers to isopropyl isomers, where branched structural isomers are characterized by a methyl substituent at the second-to-last carbon of the perfluorinated chain. Except for PFOS, PFOA, and PFOSA, the designation "iso" will be applied to the corresponding Br-isomers of other PFAS.

Quantification of individual Br-isomers was initially reported around 2005 due to the lack of commercially available standards.[29,73] Subsequent studies introduced various approaches to address this gap. Some researchers estimated isomer ratios using relative peak areas.[62,71] Semi-quantitative methods included calibration against the respective L-isomer, assuming uniform ionization efficiencies across all isomers.[66,72,74,79,87,96] Recent studies have employed quantification of Br- and L-isomers of PFOS and PFOA using isomer-specific calibration curves.[39,40] When calibration curves were generated for individual isomers, Br-PFOS consistently showed ionization efficiencies that are 2–5 times higher than L-PFOS in electrospray MS.[40] These findings highlight the importance of using the corresponding isomer for accurate quantification of each individual isomer, as previous measurements may have underestimated Br-isomers while overestimating the linear form. However, to date, enriched individual isomers are commercially available only for PFOS and PFOA.

6. PFAS isomers in aquatic biota

Studies on PFAS in aquatic organisms, examining accumulation, trophic transfer, and elimination dynamics, have consistently demonstrated that L-PFAS exhibit higher bioaccumulation factors compared to their Br-isomer counterparts. Additionally, it has been shown that Br-isomers are eliminated from the body more quickly than L-isomers.[30,66] These differences in bioaccumulation and depuration rates underscore the structural influence on uptake and retention in aquatic biota. A detailed summary of the studies reviewed in this paper is provided in Table 1.

6.1 Legacy PFAS in aquatic biota

6.1.1 PFOS. In this review, concentrations of L- and Br-PFOS (ng g^{-1}) in aquatic biota were compiled from published studies and are presented in Fig. 5. The dataset encompasses a broad range of organisms, including aquatic invertebrates, fish, seals, sharks, cetaceans (whales, dolphins, porpoises), polar bears, and seabirds/aquatic birds (egg samples). As shown in Fig. 5, across a wide range of studies, L-PFOS consistently dominates the T-PFOS burden in aquatic biota, often comprising over 88% of the isomeric mixture.[41,42,47,61,65,71,72,99,105] The organisms sampled from Lake Ontario exhibited L-PFOS proportions ranging from 88–100%, with the remainder attributed to Br-PFOS.[47] Similar dominance was observed in fish from the Labe River, Czech Republic (98–100%),[99] Sweden (92%),[111] and Eastern Red Sea near Jeddah, Saudi Arabia (96% in liver and ~90% in muscle tissues).[69] Further findings on fish,[44,67,75,112] crab,[75] and seals (96%)[62] confirm the higher abundance of the L-isomer relative to Br-isomers. Isomeric analysis of food matrices revealed L-PFOS enrichment in fish (85%), meat (63%), and vegetables (56%), with minor contributions from P3 + P5 (7%), P6 (6%), P4 (2%), P1 (1%), and P2 (~0%).[101]

In Georgia, US, aquatic wildlife exhibited 77–89% L-PFOS and 11–23% Br-PFOS, with 86% of fish analyzed containing detectable Br-isomers; the highest Br-PFOS levels were found in catfish liver, and the lowest occurred in tomtate muscle.[65] High proportion of L-PFOS (93%) was reported in European chub from the Orge River near Paris.[84] In herring muscle, L-PFOS contributed >90% of T-PFOS,[44] a pattern discovered in other fish species globally.[26] Houde *et al.*[47] reported L-PFOS levels of 88–93%, with no significant change in L-PFOS over time.

Interestingly, PFOS isomer abundance varied across water bodies in China. Tangxun Lake showed a higher proportion of Br-PFOS (21%) compared to Xiaoqing River (11%), although the relative order of individual isomers remained consistent (L- > P6 > P4 + P3 > P5 > P1).[78] Notably, Br-isomers (except P1) were more efficiently transferred to bile of crucian carp than L-PFOS, and P6, P4 + P3, and P5 were strongly associated with each other. In crucian carp gonadal tissues, P6 (43%) slightly exceeded L-PFOS (38%), followed by P5 (36%), P4 + P3 (37%), and P1 (35%).[78] The higher proportion of Br-PFOS in carp may reflect their benthic lifestyle, as recent studies have shown dis-

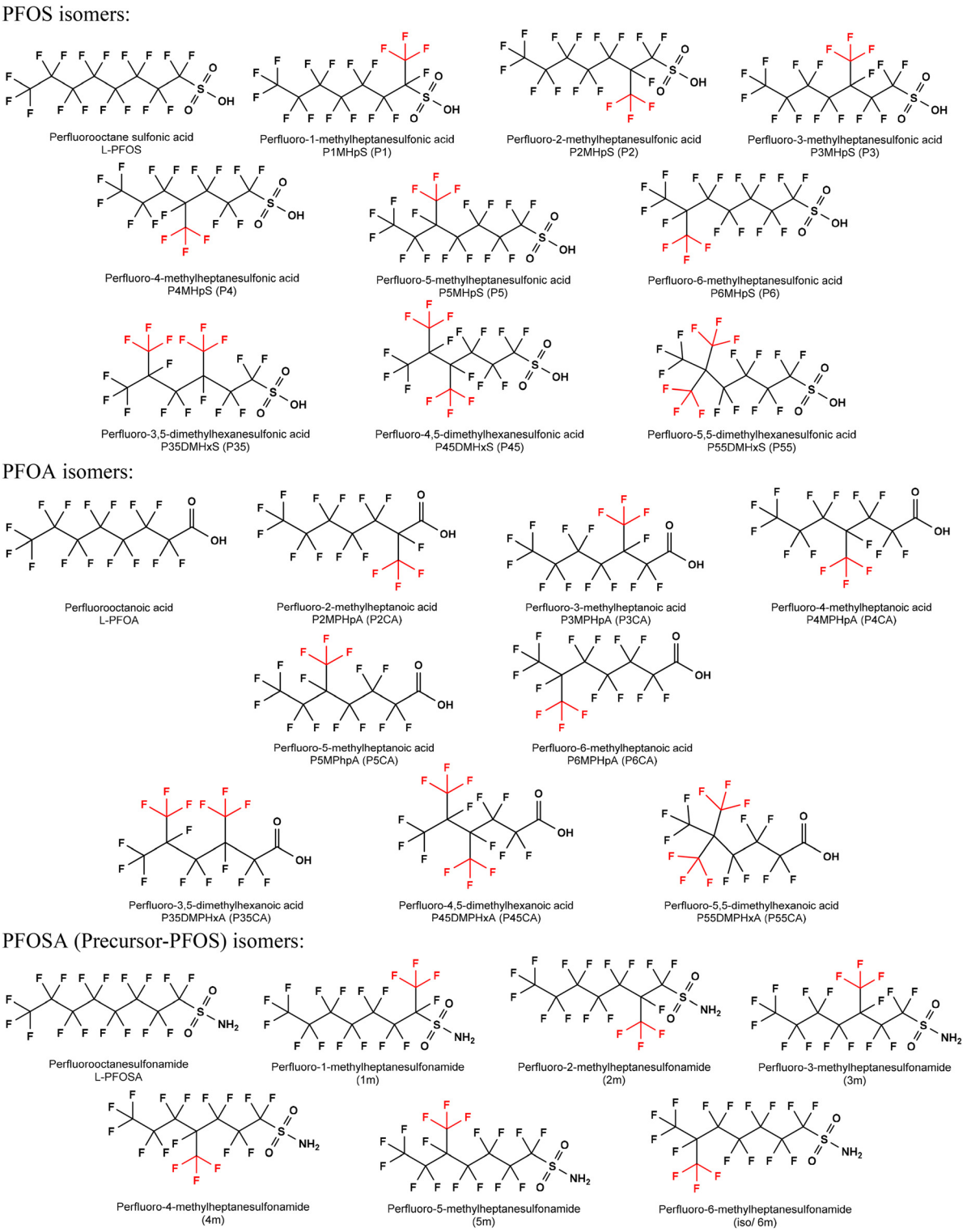

Fig. 4 Perfluorooctane sulfonic acid (PFOS) and perfluorooctane carboxylic acid (PFOA) and precursor PFOS: perfluorooctanesulfonamide (PFOSA) isomer structures with their names and abbreviations.

tinct bioaccumulation patterns in benthic fish.[39] Analyses of food samples from Beijing demonstrated L-PFOS enrichment, with Br-isomers occurring at low levels in fish.[106] Concentrations of both L and Br-PFOS were generally higher in freshwater fish than in marine species.[106] In freshwater fish, mean concentrations were L-PFOS = 451, P3 + P4 = 23, P5 = 12, and P6 = 31 ng g^{-1} ww, whereas marine fish had mean concentrations of, L-PFOS = 444, P3 + P4 = 8, P5 = 8, and P6 = 17 ng

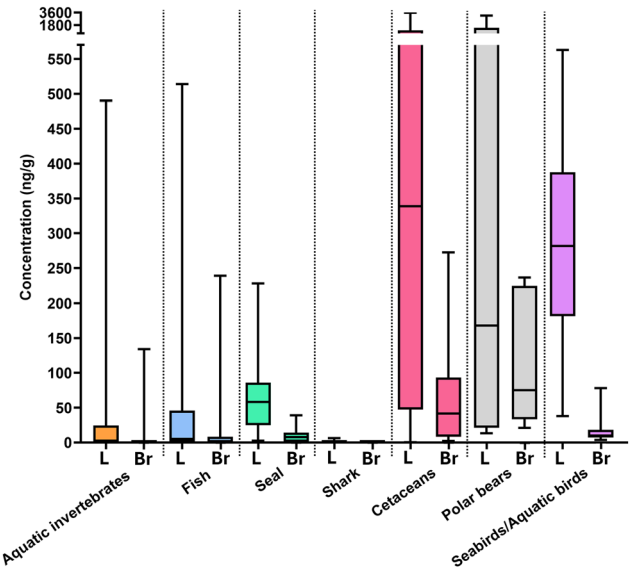

Fig. 5 Distribution of linear (L-) and branched (Br-) PFOS concentrations (ng g^{-1}) in aquatic biota, compiled from research papers included in this review. Concentrations are summarized across major groups, including aquatic invertebrates, fish, seals, sharks, cetaceans (whales, dolphins, porpoises), polar bears, and seabirds/aquatic birds (egg samples). The concentration of L-PFOS ranged from 0.11–3574.2 ng g^{-1} while Br-PFOS ranged from 0.02–272.5 ng g^{-1}. The data highlight the predominance of L-PFOS relative to Br-PFOS across these groups. We compiled and graphed the reported concentrations of L- and Br-PFOS from studies that quantified these isomers separately. Only publications analyzing wild-caught or market-purchased aquatic biota were included, while controlled exposure studies were excluded.

g^{-1} ww. Br-PFOS represented 12.7% of T-PFOS in freshwater fish, and 6.8% in marine fish. Habitat-related differences were evident in shark species, with Caribbean reef sharks showing lower L-PFOS (79 ± 8%) compared to New York Bight sharks (93 ± 7%).[60] In European waters, PFOS was detected in all fish samples, with L-PFOS varying geographically from 95 ± 2% in the Bothnian Bay and Kattegat to 77–89% in the Northern and Southern Baltic Proper.[85]

A recent review summarized global PFAS contamination in seabird populations and noted the presence of both L- and Br-PFOS.[113] However, several species show divergent isomer patterns. For example, analyses of penguins detected only L-PFOS, with no evidence of Br-PFOS.[102,108] In herring gull and double-crested cormorant eggs, a study reported strong dominance of L-PFOS (94.5% and 95.9%, respectively), and the presence of mono-PFOS isomers in all samples.[92] Subsequent investigations consistently confirmed L-PFOS dominance, including 95.0–98.3% in herring gull eggs,[98] 81.5% in guillemot eggs,[84] and 88.5% in double-crested cormorant eggs.[40] Mono-PFOS profiles typically followed the pattern P6 > P5 > P4 > P3 > P2 > P1, although more recent work reported a shift toward co-eluting P3, P4, P5 > P6 > P1.[92,98] While earlier studies did not detect di-PFOS isomers,[92] later analyses reported their presence in more than 60% of herring gull egg samples across multiple sites.[98] Detected di-PFOS included P35 and P45 in Toronto Harbor (Lake Ontario), P35 in Chantry Island (Lake Huron) and Fighting Island (Detroit River), and P45 in Gull Island (Lake Michigan).[98] The most recent study of double-crested cormorant eggs from Buffalo Harbor (NY, USA) reported 1.2% of the unseparated P35, P45, and P55 di-PFOS isomers.[40] Another recent investigation of seabirds found high proportions of L-PFOS (~74%) in black-browed albatrosses, common diving petrels, and white-chinned petrels from 2004 to 2014.[110] Notably, Br-PFOS were increased ~15–20% in white-chinned petrels and common diving petrels collected at South Georgia in 2014 relative to earlier years, although 2014 data for black-browed albatrosses were not available.

6.1.1.1 Bioaccumulation and trends. Multiple studies have demonstrated that L-PFOS accumulates more readily in aquatic organisms than its Br-PFOS counterparts.[47,62,66,72,76] Fig. 5 provides a visualization of the trophic magnification factor (TMF) involving aquatic biota, highlighting differences in the bioaccumulation of L-PFOS and Br-PFOS. Lower trophic level organisms, such as aquatic invertebrates and some fish, show lower T-PFOS concentrations, while L-PFOS remains more abundant than Br-PFOS. In contrast, higher trophic level organisms, including cetaceans, polar bears, and aquatic birds, exhibit substantially higher T-PFOS concentrations with a clear dominance of L-PFOS. In biota samples from Lake Ontario, six PFOS isomers were identified: three mono-PFOS, three di-PFOS, and L-PFOS.[47,77] The predominance of L-PFOS suggests either reduced uptake, faster elimination, selective retention of Br-isomers, or a combination of all these factors.[47] This trend was similarly observed in the guillemot food web,[84] where L-PFOS concentrations increased from prey to predator, indicating preferential trophic biomagnification of this isomer.[84,114] Another study focusing on adult eastern oysters also reported that L-PFOS was present at high levels, whereas the Br-isomer had been almost eliminated from the tissue.[80]

PFOS isomer patterns in the biota closely resembled those in sediment samples, even among pelagic organisms such as zooplankton, suggesting strong partitioning of L-PFOS to both sediment and biota.[47] L-PFOS exhibited a trophic magnification factor of 4.6, which was higher than that observed for the mono-PFOS isomers (ranging from 1.3 to 2.6). In contrast, di-PFOS showed no evidence of biomagnification. L-PFOS was the dominant isomer in zooplankton, Mysis, and Diporeia, whereas mono-PFOS appeared at low levels.

Benthic organisms, such as polychaetes, crabs, Diporeia, and sculpin (a benthic fish), exhibited isomer patterns closely resembling those observed in the sediment, with pronounced enrichment of L-PFOS compared to pelagic species.[39,47,70] Sediment appears to act as a reservoir for L-PFOS, facilitating its uptake by benthic organisms and contributing to contamination at higher trophic levels.[39,47,70,72] Within fish species, mono-PFOS isomers were more abundant than in invertebrates, with the co-eluting P3/P4/P5 isomers being the most frequently detected. In contrast, P1 and P6 were present at much lower concentrations. Di-PFOS isomers were detected at low levels in only a few fish species, including smelt and sculpin.[47] Overall, these patterns suggest that both L-PFOS and

mono-PFOS undergo biomagnification within the Lake Ontario food web. Moreover, both L- and Br-PFOS were higher in benthic than in pelagic fish, and the lack of isomers in pelagic fish reinforces the role of sediment-associated pathways.[39] Additionally, the elevated Br-PFOS levels observed in lower-trophic organisms are hypothesized to reflect exposure to Br-PFOS precursors. Previous studies have shown that these Br-precursors undergo faster biotransformation than their L-counterparts, leading to an enrichment of Br-isomers.[115]

A study showed that the proportions of Br-PFOS isomers detected in fish (50%) and seal tissues (4%) differed significantly.[62] While Br-PFOS were absent from ringed and bearded seal blubber, the blood and liver samples from these species contained the 4% Br-isomers. The authors of the study attributed these observed results to differences in depuration rates, suggesting that Br-PFOS isomers are eliminated more quickly than linear PFOS in seals, especially when Arctic cod makes up a major part of their diet.[62] Overall, cod and seals showed a predominance of L-PFOS, ranging from 50% to 96%.[62] Feeding behavior further influenced the abundance of L-isomers: zooplankton feed exclusively on phytoplankton, Mysis consume phytoplankton, sediment/detritus, and zooplankton, while Diporeia primarily feed on sediment/detritus.[116] Despite the lack of sediment contact, zooplankton exhibited similar isomer patterns to Diporeia, suggesting indirect exposure through food sources.

In laboratory studies, isomer-specific biological discrimination and maternal transfer of PFOS isomers have been demonstrated for the first time using rainbow trout and zebrafish eggs.[66] In this study, despite exposure to a known isomeric mixture, stereoselective bioaccumulation of Br-isomer contents in tissues were observed, with the liver showing the highest accumulation. The relative bioaccumulation efficiency of Br-isomers followed the order: P1 > P6 > P5 > DM2 > P4 > P3 > DM1 > DM3, with subtle tissue-specific variations in the liver and kidney. This study showed that analysis of exposed trout tissues indicated preferential elimination of Br-PFOS through the kidneys and gills, which likely explains its reduced tissue levels. Notably, the isomers in zebrafish eggs mirrored those of adults, indicating largely non-selective maternal transfer.[66]

In aquatic environments impacted by firefighting foam, biota generally showed enrichment of L-PFOS, although proportions varied by species and trophic level. Fish liver samples from contaminated lakes contained 87–90% L-PFOS, with P6 (~5%) and P3/P4/P5 as the dominant Br-isomers.[75] In contrast, aquatic invertebrates exhibited higher Br-PFOS proportions (15–28%),[67] although Koch *et al.* reported slightly lower values (0–20%).[86] Findings from the Lake Ontario fishes and invertebrates demonstrated significant differences in L-PFOS percentage composition across species.[72] Lake trout have exhibited isomers similar to those of their prey, indicating that diet is a key driver of accumulation.

Relative to other aquatic biota, marine mammals exhibited elevated concentrations of both L- and Br-PFOS (Fig. 5), although L-PFOS was consistently the predominant isomer accumulated. Pilot whale liver samples collected between 1984 and 2006 showed relatively stable isomer profiles, whereas ringed seals exhibited a gradual decline ($P < 0.01$) in L-PFOS from 91% (in 1984) to 83% (in 2006) over the same period.[76] Br-isomers were lower in whale livers (6–7%) compared to seal livers (9–17%).[76] Similar observations were observed in a study of polar bears from East Greenland,[42] Canadian Arctic (Nunavut), and Svalbard, Norway.[92] L-PFOS comprised 93.0% (East Greenland),[42] 92.4% (Canadian Arctic)[92] of T-PFOS isomers in liver tissue, while its proportion was significantly lower in blood samples at 85.4% ($p < 0.05$, East Greenland)[42] and 82.4% (Svalbard, Norway).[92] Across both matrices, the Br-isomer P6 emerged as the predominant Br-PFOS, while none of the di-PFOS were detected.[42,92] Another study showed similar abundance of L-PFOS in polar bears and killer whales: 88.4% and 89.9% respectively, while significantly higher ($p < 0.001$) L-PFOS in ringed seals (92.1%).[87]

In Taihu Lake, China, across various tissues including muscle, gill, kidney, liver, and eggs showed that L-PFOS was the predominant isomer (47%–97). Br-isomers followed a consistent pattern: P3 + P5 > P4 > P6 > P1 > P2: (range ~0–4%), with a slight deviation in muscle where P2 exceeded P1.[67] This differs from the later study[100] but aligned with the Houde *et al.* findings (P6 > P3 + P4 + P5 > P1 > P2).[47] P2 consistently showed the lowest uptake and shortest half-life in lake trout,[66] while P1 demonstrated the highest absorption and longest retention, contributing to its elevated presence in biota despite low water concentrations.[66,67] L-PFOS was most abundant in *Pelteobagrus fulvidraco* (yellowhead catfish) and lake saury, followed by mono- and di-PFOS.[67] Abundant L-PFOS in liver and kidney reflected its lower excretion rates[67] observed in zebrafish and rainbow trout.[66] The L-PFOS were >85% in all taxonomic groups: fish, crustaceans (shrimp and crab), and cetaceans (finless porpoises and Indo-Pacific humpback dolphins) from the northern South China Sea.[45] The trophic magnification followed the order: L-PFOS > P6 > P5 > P4 > P3, which was consistent with the order of their log K_{ow}.[46,73]

In fish, L-PFOS accumulated to a greater extent than Br-isomers, driven by higher uptake rates and slightly lower elimination rates, resulting in higher bioaccumulation[30,81,103] like in the exposure study done with the carp, where they found uptake rates following the order: L-PFOS > P1 > P4 > P3 + P5 > P2, while L-PFOS was preferentially accumulated.[100] L-PFOS also exhibited stronger partitioning from blood to other tissues, resulting in lower blood concentrations compared to Br-PFOS.[100] Br-isomers were more readily eliminated *via* the kidney and gill, and tended to partition into blood more than L-PFOS. Another study showed that L-PFOS was predominantly excreted *via* feces, while Br-isomers were preferentially eliminated through urine.[103] The highest PFOS concentrations were detected in blood (B), followed by kidney (K) > liver (L) > muscle (M), consistent with patterns reported in a previous study.[67] The tissue-to-blood ratios (M/B, L/B, and K/B) for L-PFOS were 0.095, 0.397, and 0.422, respectively. Other Br-PFOS isomers exhibited a similar trend, with ratios increasing in the order M/B < L/B < K/B.

Cross-boundary transfer of PFOS isomers from aquatic environments to riparian zones *via* emergent insects has shown aquatic insect and invertebrate groups exhibiting significantly lower proportions of Br-PFOS (<18%), indicating that L-isomers were enriched in biota.[104] This enrichment is likely driven by the faster elimination rates of Br-isomers, as previously reported.[47,117,118] The long-term monitoring of PFOS isomers in grey seals from the Baltic Sea, over a period of 35 years (1974–2008)[71] has conducted, although they did not quantify the Br-PFOS. This study showed that although L-PFOS is prevalent, the contribution of Br-isomers increased over time, 1974–2005 (7–22%), with the highest content observed between 2004 and 2006.[71] They also suggested that the increasing proportion of Br-isomers over time may be attributed to their shorter blood depuration half-lives compared with the corresponding linear isomer. However, Br-PFOS concentrations declined following the 3M phase-out.[29,44,99]

6.1.1.2 Biotransformation. Biotransformation of PFOS precursors (Pre-PFOS), particularly PFOSA[30] and (*N*-ethyl perfluorooctanesulfonamido)ethanol-based phosphate diesters (diSPAP),[31] plays a significant role in environmental PFOS levels. A summarized schematic diagram of the biotransformation of Pre-PFOS is shown in Fig. 6. PFOSA and diSPAP contain the PFOS substructure, as illustrated in Fig. 6. These compounds have been introduced as PFOS equivalents, and their manufacturing processes also generate isomeric by-products.[71,119] Studies show that Br-isomers are preferentially metabolized and accumulated, especially Br-diSPAP, leading to notable enrichment of Br-PFOS in medaka.[31] Their proposed transformation pathways have been proposed in the publication by Peng *et al.*[31] L-PFOS levels were lower when exposed to diSPAP compared to the technical PFOS standard, confirming the conversion of diSPAP to PFOS.[31] Moreover, mono-PFOS exhibited greater enrichment and biomagnification in food webs than L-PFOS.[31,47]

Br-PFOSA isomers also undergo preferential metabolism to Br-PFOS, resulting in pronounced accumulation of Br-PFOS in fish tissues over L-PFOSA,[30,107,120] most notably in liver, followed by blood ≈ kidney > muscle.[30] The transformation of PFOSA to PFOS isomers typically follows the order P1 > P6 > P3 + P4 + P5, [30] while biotransformation of L-PFOSA to L-PFOS is slower. Direct PFOS exposure provided the opposite trend in isomer profile (P6 < P3 + P4 + P5 ≈ L- < P1).[77] Elimination behavior of P1 varies across studies, being either the slowest or fastest-cleared isomer. P1 showed variable elimination behavior across studies, ranging from the most slowly eliminated isomer[114,121–123] to the fastest.[30,107,120] PFOS elimination rates followed L- < di-PFOS < mono-PFOS, with faster clearance of

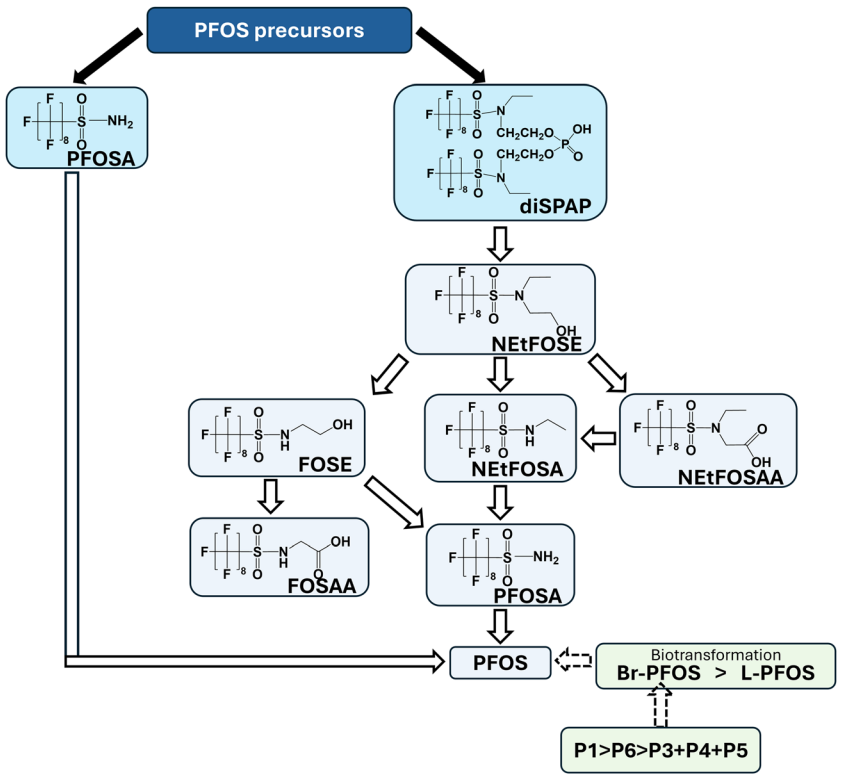

Fig. 6 Summary of proposed biotransformation pathways from PFOSA and diSPAP to PFOS isomers from published work reviewed. PFOS (perfluorooctane sulfonic acid), PFOSA (perfluorooctanesulfonamide), diSPAP ((*N*-ethyl perfluorooctanesulfonamido)ethanol-based phosphate diesters), NEtFOSE (*N*-ethyl-*N*-(2-hydroxyethyl)perfluorooctylsulfonamide), FOSE (perfluorooctanesulfonamido ethanol), NEtFOSA (*N*-ethylperfluorooctanesulfonamide), NEtFOSAA (2-(*N*-ethylperfluorooctanesulfonamido)acetic acid), P1, P3, P4, P5, P6 (names of each isomer in this figure can be found in Fig. 4). Br- (branched), L- (linear). Dotted arrows with light green boxes include more isomer details about the produced PFOS.

Br-isomers likely due to their lower hydrophobicity[30,107] following the order L- < P3 + P4 + P5 < P6 < P1,[77] which could well explain the faster rate of elimination of Br-isomers through fish gill or/and urine.[117] Metabolism predominantly occurred in the liver rather than the kidney,[30] and co-exposure to PFOSA does not significantly influence PFOS depuration from blood.[77]

6.1.2 PFOA. Among aquatic biota, PFOA is the second most frequently detected PFAS, with the L-isomer comprising more than 90% of T-PFOA across taxa (Fig. 7); in contrast, Br-PFOA isomers are rarely detected.[39,41,90,101,109] A study with liver samples of polar bears from Greenland revealed a diverse array of Br-PFCA (Br-perfluoroalkyl carboxylic acids) isomers, in contrast to Canadian specimens, where only L-PFOA was detected.[97] Br-PFOA isomers, when present, occur at significantly lower concentrations than in technical ECF PFOA mixtures. In Lake Ontario biota,[90] eight PFOA isomers were separated, with P5CA and P6CA detected in Mysis, sculpin, Diporeia, alewife, and smelt, while P3CA was observed in select sculpin, smelt, and composite Diporeia samples. The presence of isomers in sediments closely mirrored those found in Diporeia, suggesting sediment-biota transfer.[90] Bottlenose dolphin blood samples revealed L-PFOA alongside Br-isomers P3CA, P4CA, P5CA, and P6CA, with P6CA being most abundant, while Br-PFOA were not detected in ringed seals.[90] However, in the northern South China Sea, Br-PFOA were only detected in cetacean liver samples, comprising less than 1% of T-PFOA.[45]

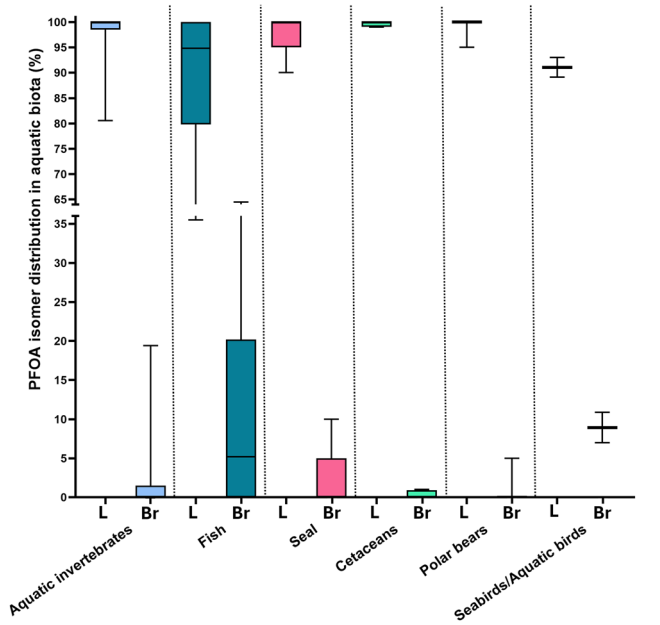

Fig. 7 Percentage distribution of branched (Br) PFOA and Linear (L) PFOA across the publications on aquatic biota reviewed, displaying that L-PFOA consistently dominates over Br-PFOA isomers. Distribution percentages are summarized across major groups, including aquatic invertebrates, fish, seals, cetaceans (whales, dolphins, porpoises), polar bears, and seabirds/aquatic birds. As fewer studies have quantified individual PFOA isomers compared to PFOS isomers, the percentage distribution of T-Br-PFOA isomers and L-PFOA were considered. Data from controlled exposure studies were excluded.

Human dietary exposure studies further confirmed L-PFOA enrichment in fish,[101,106] shrimp,[45,67] and shellfish,[41] with no Br-PFOA detected in food samples from Beijing.[76] Another study has shown enrichment of 94% of L-PFOA in clam meat.[109] Enrichment of L-PFOA might also be due to the production of PFOA by telomerization.[67] The presence of Br-isomers such as P6CA, P4CA, and P5CA in fish align with previous reports,[67,73,117] although lower detection of P6CA and P5CA may reflect reduced bioaccumulation or enhanced elimination, as noted by De Silva *et al.*[91] A recent study employing cIMS confirmed L-PFOA in all the tested market samples, including blue catfish, cod, haddock, rainbow trout, and tilapia.[39] Co-eluting Br-isomer peaks (P3CA + P6CA and P4CA + P5CA) were also detected; however they were notably absent in two salmon species. No significant differences in isomer profiles were observed between pelagic and benthic fish due to the higher hydrophilicity of the isomers.[39]

6.1.2.1 Bioaccumulation and trends. Multiple studies have demonstrated that L-PFOA is preferentially bioaccumulated in aquatic organisms across diverse ecosystems (Fig. 7).[41,45,67,90,91] The consistent detection of Br-PFOA isomers, albeit at lower concentrations, similar to Br-PFOS, suggests that environmental PFOA originates primarily from ECF processes.[26,67,73,101] In contrast to PFOS, both L-PFOA and its Br-isomers were found at comparable concentrations across different fish species, suggesting that PFOA's higher water solubility facilitates a more uniform distribution of its isomers throughout the water column.[39]

In rainbow trout, toxicokinetic analysis revealed that L-PFOA and PFOA-8 exhibited the highest accumulation, having the largest half-life among eight detected isomers, with L-PFOA enriched across all tissues.[91] P6CA displayed the shortest half-life, where it is different from Taihu Lake findings[67] in which P6CA was the most accumulated Br-isomer, suggesting species-specific elimination mechanisms. Additionally, PFOA-7 was present in the administered dose but undetectable in tissues, indicating rapid elimination or poor tissue partitioning.[91] Tissue-specific distribution showed higher L-PFOA concentrations in the heart and spleen compared to liver, blood, and kidney, and overall faster clearance of Br-isomers than linear forms.[91]

A study from Taihu Lake, China,[67] confirmed L-PFOA as the dominant isomer in all tissues and eggs of sampled aquatic organisms, like in most biota samples in North America[90] and biota in the Western Arctic food web,[62] with gills containing relatively lower levels.[67] Interestingly, despite its frequent detection, P6CA has shown rapid elimination in fish, as in the early study,[91] while P4CA and P5CA were the least abundant isomers.[67] Invertebrate samples from Taihu Lake exhibited lower Br-isomer contributions than surface water,[79] where a similar Br-isomer pattern for PFOA was found in the food web of Lake Taihu in China.[67,117] This is likely due to the higher water solubility and reduced uptake and faster elimination of Br-isomers.[47,75] This pattern was consistent with observations

across the lake's food web, reinforcing the notion of selective retention and reduced bioaccumulation of Br-PFOA isomers in aquatic biota.

In Liaodong Bay marine species, only P6CA was detected among Br-isomers,[73] which was reasonable given that P6CA is the most prevalent Br-isomer in ECF PFOA. L-PFOA showed a positive correlation with trophic level, and trophic magnification factors (TMFs) > 1 confirmed its biomagnification potential. This trend likely reflects the preferential bioaccumulation and slower elimination of L-PFOA compared to Br-isomers.[73,91,114,121]

A comprehensive tissue distribution study reported the isomers: L- > P6CA ≥ P3CA > P5CA ≥ P4CA in carp.[78] Br-isomers were consistently less bioaccumulative than L-PFOA, except in bile, where Br-isomer-specific transfer was more pronounced. These findings suggest distinct partitioning and excretion pathways for Br-isomers.[78]

6.2 Other PFSA isomers

6.2.1 PFOS precursor isomers. As PFOS is the major PFAS known to have isomers, studies were conducted on Pre-PFOS isomers to understand the PFOS isomer distribution. Longitudinal monitoring of grey seal liver from the Baltic Sea (1974–2008) revealed a distinct temporal shift in PFOSA isomer composition.[71] While L-PFOSA consistently dominated, the proportion of Br-PFOSA increased markedly between 1969 and 2004 (2–28%). Despite this rise, multiple studies have shown preferential accumulation of L-PFOSA over Br-isomers across species, with L-PFOSA exhibiting longer half-lives and greater tissue retention.[30,31,85,100,117,120,124] As an example, a study has shown the Br-PFOSA decreased between 1991 and 2011 (10 to <3%),[44] suggesting Br-PFOSA was preferentially eliminated and/or biotransformed in the fish.[30,31] In Crucian carp from China, both L- and Br-PFOSA were detected in over 80% of tissue samples, though Br-isomers were present at lower proportions (6.6–11.6%), with no significant differences among tissues.[78] A strong positive correlation between L-PFOS% and L-PFOSA% suggests that PFOSA may serve as a precursor contributing to PFOS levels.[31,72] Among the biota matrices, except for L-PFOSA in the zooplankton (55%), Br-PFOSA was detected in high amounts (significantly in herring and sprat).[84] Interestingly, L-PFOSA percentages declined with increasing trophic level,[84] potentially due to faster uptake of Br-FOSA[31] and more rapid elimination of L-PFOSA,[123] but in contrast to the faster biotransformation of Br-PFOSA to Br-PFOS.[120] A tissue-specific accumulation showed lower %Br-PFOSA among tissues, ranging from the lowest 7% in the kidney to the highest 12% in the liver, but there were no statistically significant differences among the tissues.[30]

In controlled exposure studies, L-PFOSA was slightly enriched in fish blood (78%) relative to the exposure solution (76%), while Br-isomers were proportionally depleted.[107] The rank order of detected isomers were 1m- < 3 + 4 + 5m- ≈ 6m < L-PFOSA (isomers structures can be found in Fig. 4), highlighting the highest accumulation potential for L-PFOSA and the lowest for 1m-PFOSA.[107]

Geographically, L-PFOSA concentrations were notably higher in the Kattegat (96%) than in the Baltic Sea (63–74%), potentially reflecting regional differences in exposure or transformation rates.[85] Elevated salinity in marine environments may inhibit L-PFOSA degradation, whereas biotransformation of PFOS precursors proceeds more rapidly in freshwater systems.[85,125–127] Furthermore, a contribution of <15% of Br-PFOSA to the T-PFOSA was observed in edible fish (burbot, pike, perch, pike perch, brown trout, salmon, and whitefish) from Lake Vättern in Sweden and from the Baltic Sea[128] in contrast to the previous study.[85] The first study of PFOSA isomers on Greenland marine mammals has shown that polar bears contained significantly higher ($p < 0.002$) L-PFOSA (98.5%) than in ringed seals (95.0%) and killer whales (94.4%).[87] These findings claim that carnivora species have a much higher capacity to transform PFOSA to PFOS compared to cetacean species.[87,129]

Biotransformation of diSPAP to PFOS involved multiple intermediates that were detected exclusively in exposed fish, including PFOSA, *N*-ethyl perfluorooctanesulfonamide (NEtFOSA), 2-(perfluorooctanesulfonamido)acetic acid (FOSAA), *N*-ethyl 2-(perfluorooctanesulfonamido)acetic acid (NEtFOSAA), FOSE, and (*N*-ethyl perfluorooctanesulfonamido)-ethanol (NEtFOSE).[31] Several isomeric forms of PFOSA, FOSAA, and NEtFOSAA were observed, supporting the hypothesis of branched-isomer-biased metabolism and subsequent enrichment of Br-PFOS in medaka. The faster elimination of Br-PFOSA compared to L-PFOSA further supports its preferential metabolism to Br-PFOS.[31]

Isomer-specific environmental behavior of perfluoroalkyl sulfonyl fluorides (PFASFs) was reported for the first time, with detected compounds such as perfluoropentane sulfonyl fluoride (PFPeSF), perfluorohexane sulfonyl fluoride (PFHxSF), perfluoroheptane sulfonyl fluoride (PFHpSF), perfluorooctane sulfonyl fluoride (PFOSF), and their isomers.[43] Freshwater fish from the Wangyu River exhibited enrichment of L-PFASF, with Br-isomers comprising 16–25% of T-PFASFs.[43] Bioaccumulation increased with carbon chain length for both L- and Br-forms. Shorter-chain L-PFASFs were more hydrophilic and rapidly excreted, while Br-isomers were less accumulated relative to their linear counterparts. Notably, L-PFOSF concentrations in fish correlated significantly with PFOS levels.[43]

6.2.2 Other PFSA isomers. Studies have shown that L-PFSAs were preferentially accumulated than Br-PFSAs in fish (carp, PFHxS),[103] aquatic insect and invertebrate (PFHxS),[104] invertibrates (PFHxS and PFHpS),[79] and Lake Ontario trout (PFDS),[77] which was in accordance with that of PFOS isomers.[103,130] Notably, L-PFHxS was primarily excreted in urine, whereas Br-PFHxS was more prevalent in feces, contrasting with the elimination patterns of PFOS isomers.[103] Further, a recent research has shown the presence of unsaturated PFOS and new isomers of Nafion Byproduct (NB2) in alligator blood from North Carolina.[95]

6.3 Other PFCA isomers

In addition to PFOA isomers, a variety of PFCA isomers have been detected in aquatic biota worldwide. A study with polar

bears from the Canadian Arctic and eastern Greenland has shown that for longer-chain PFCAs, such as PFNA and perfluorotridecanoic acid (PFTriDA), both regions exhibited a predominance of L-isomers, exceeding 99% of the total composition.[97] Interestingly, branched variants of perfluorodecanoic acid (PFDA), perfluoroundecanoic acid (PFUnDA), and PFDoDA were present in polar bear liver samples.[97] These findings point to a likely influence from ECF processes, known for producing mixtures of L- and Br-isomers. Early work in Lake Ontario provided the first temporal analysis of Br-PFCA isomers in biota (1979–2004), with isomers of PFUnDA[29,77] and PFTriDA[29] detected in lake trout from the Niagara River. Over time, the prevalence of L-isomers increased, reflected by rising linear-to-branched peak area ratios. Around 1988, coinciding with the phase-out of ECF-based PFCAs production in North America, Br-isomer concentrations began to decline, reaching trace levels by 2004. This shift indicated reduced emissions or decreased use of isomer-containing products, with later inputs likely originating from telomerization processes that produce L-PFAS exclusively.[29]

Dolphin blood samples from North American environments contained multiple Br-PFNA isomers consistent with an ECF profile, with PFNA-4 and isopropyl (iso)-PFNA being the most prevalent.[90] Iso-PFUnDA was the most prevalent isomer, followed by PFDoDA, while iso-PFDA occurred in small proportions. In ringed seals, Br-PFNA consisted solely of iso-PFNA, with iso-PFDA and PFUnDA also detected. In Lake Ontario biota (smelt, sculpin, and Diporeia), only L- and iso-PFNA were detected, with iso : L ratios showing non-significant variability (0.41–0.57%). Ringed seals from Resolute Bay contained only iso-PFNA among branched forms, while iso-PFNA was detected in just one of the polar bear liver samples at the limit of detection. The iso : L-PFNA ratios were 0.3% in ringed seals and 0.4% in polar bears.[90] Further, a recent study has shown the presence of an isomer of PFUnDA in alligator blood.[95]

Beyond North America, PFCA isomer distribution in Liaodong Bay, China, showed L-PFUnDA, L-perfluorododecanoic acid (L-PFDoDA), L-PFTriDA, and L-perfluorotetradecanoic acid (L-PFTeDA) at the highest concentrations in China anchovy livers, with much lower levels in muscle.[73] In invertebrates, longer-chain PFCAs occurred at much lower levels compared to fish. Only the iso-isomer was observed from PFDA to PFTeDA in fish livers. Iso-PFCAs of even carbon numbers are consistently more abundant than the preceding odd-numbered iso-PFCAs, which is opposite to the trend in L-PFCAs reported for Chinese sturgeon.[131] This even–odd abundance pattern for iso-PFCAs has also been reported in Arctic seals.[132] Among aquatic samples, iso-PFDoDA and iso-PFTeDA were detected with frequencies of 44% and 55%, respectively.[73] In contrast, iso-PFDA was only detected in redeye mullet and half-smooth tongue-sole, iso-PFUnDA and iso-PFTriDA in Japanese Spanish mackerel, iso-PFDoDA in rock shell, and iso-PFTeDA in Chinese mitten-handed crab.[73]

6.3.1 Bioaccumulation and trends. In rainbow trout, L-PFNA accumulated to higher levels than Br-isomers across all examined tissues: blood, liver, kidney, heart, and spleen, with the longest half-life observed for L-PFNA, followed by iso-PFNA.[91] The heart and spleen showed greater enrichment of L-isomers compared to the liver, blood, and kidney. This study showed Br-isomers were cleared more rapidly relative to L-isomers.[91] In a marine food web study from Liaodong Bay, China, L-PFCAs exhibited a clear trophic-level-dependent increase, with higher proportions in fish than invertebrates.[73] Invertebrates generally showed lower concentrations of L-PFCAs, with the lowest levels of all L-PFCAs found in the short-necked clam, which occupied the lowest trophic level in the studied food web. All L-PFCAs showed significant positive correlations with trophic level, and TMFs exceeded 1, indicating biomagnification. TMFs of iso-PFCAs were also reported for the first time, and the relatively higher biomagnification of L-isomers suggests preferential production of L-PFCAs from fluorotelomer alcohol (FTOH) metabolism.[133,134] Overall, this study provided the first detailed characterization of isomer-specific trophic transfer of PFCAs in a marine food web,[73] revealing patterns similar to PFSAs, where L-isomers undergo biomagnification as discussed above. There are studies targeted the PFCA isomers, where they were not detected,[71,75,76] while a study reported PFCAs might not accumulate in fish.[75]

6.4 Other PFAS isomers: enantiomers

In the literature, PFAS research has examined not only constitutional/positional isomers, which share the same molecular formula but differ in the connectivity of their atoms, but also stereoisomers, which possess identical formulas and connectivity yet vary in their three-dimensional arrangements. Within the category of stereoisomers, researchers have focused on both enantiomers, which are mirror-image forms that cannot be superimposed, and diastereomers, which differ in spatial configuration but are not mirror images.

The enantiomeric analysis on P1 PFOS isomers (structures shown in Fig. 8) has revealed further biological discrimination: zooplankton showed enrichment of one enantiomer while Diporeia and mysids favored the opposite enantiomer, implying species-specific biotransformation pathways.[72] While sculpin and rainbow smelt showed a racemic mixture of PFOS, a nonracemic mixture is observed in the top predators, such as lake trout, and all invertebrate species. Interestingly, forage fish generally matched racemic standards, though some species displayed isomer ratios inconsistent with their known prey, suggesting additional ecological or metabolic influences.[72] For the first time, a study measured the cis- and trans-diastereomers of perfluoroethylcyclohexane sulfonate (PFECHS) in aquatic organisms (structures shown in Fig. 8).[45] Both isomers biomagnified in crustaceans, fish, and cetaceans, but trans-PFECHS showed substantially greater increases in concentration with trophic level.[45]

7. Knowledge gaps and future research directions

Although PFAS are widely recognized for their persistence, toxicity, and propensity to bioaccumulate, the environmental fate,

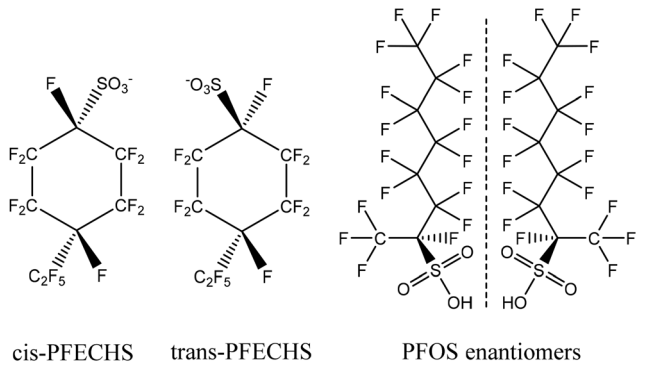

Fig. 8 Diastereomers of perfluoroethylcyclohexane sulfonate (PFECHS); *cis*- and *trans*-PFECHS isomers and enantiomers of perfluorooctane sulfonic acid (PFOS) P1MHpS/P1 isomer.

toxicological effects, and bioaccumulation behavior of individual PFAS isomers remain insufficiently characterized. Much of the existing work has focused on legacy PFAS, leaving substantial gaps in our understanding of isomer-specific behavior, particularly for emerging and replacement compounds. Toxicokinetic differences between L- and Br-isomers, such as variations in elimination rates and tissue distribution, are still poorly defined, especially for less-studied congeners. A major limitation in current PFAS research is the lack of reference standards for many isomers, which constrains accurate quantification and inter-study comparability. Analytical challenges are compounded by differences in ionization efficiencies, including the consistently higher MS response of Br-PFOS relative to L-PFOS. Future efforts should therefore prioritize the development of isotopically-labeled standards with enriched isomers and calibration strategies that mitigate the risk of underestimating branched isomers and overestimating linear forms.

Another significant barrier is the limited ability to separate, identify, and quantify individual PFAS isomers. Although GC-MS with derivatization has been used to achieve isomer separation, further methodological refinement in extraction and sample preparation is needed.[97] The integration of IMS with HRMS is a promising platform for PFAS isomer analysis, but its application remains in early development. Effective use of IMS will require optimization of instrumental parameters, including drift path length (*e.g.*, number of passes) and source conditions, tailored to specific PFAS classes.[39,40] Supercritical fluid chromatography (SFC) also represents an underexplored opportunity. While SFC has been applied to enantiomer separation,[135] no studies have yet investigated its potential to resolve PFAS constitutional isomers. Developing and validating SFC methods specifically for PFAS isomer analysis would provide an important additional tool for comprehensive isomer-specific characterization. Finally, expanded application of advanced analytical techniques, such as LC-IMS-HRMS, non-targeted analysis, and HRMS workflows, could uncover previously undetected isomers, improve our understanding of PFAS transformation pathways, and enhance source-tracking capabilities. Such advances will be essential for refining exposure assessments and supporting the development of more effective regulatory and remediation strategies.

Despite growing recognition that PFAS isomer profiles can serve as chemical fingerprints, their systematic use in source attribution remains limited. Although environmental data on isomer distributions are sparse, existing evidence demonstrates their potential to reveal contamination pathways affecting both humans, wildlife, including aquatic biota. Subtle differences in isomer signatures can distinguish residual PFOS and PFOA in consumer products manufactured before 2002 from direct emissions, while PFOS profiles may further differentiate indirect exposure *via* precursors from direct exposure to the sulfonate, supported by findings of isomer-specific biotransformation.[26] Studies have shown that the ratio of Br- to L-isomers can differentiate ECF-derived products such as legacy AFFF foams.[136] Moreover, biosolids and landfill leachates exhibit distinct isomeric fingerprints aided by perfluorosulfonamido acids and co-occurring fluorinated compounds.[137] Additionally, a tiered analytical framework has recently been explored to support source attribution by combining a screening method to assess bulk PFAS signatures, targeted compound analysis, and isomer-resolved methods. It has been applied to AFFF concentrates and food contact materials, demonstrating that this framework can be implemented in a practical, high-throughput format for source attribution.[138] With the phase-out of PFAS-based chemical production in the early 2000s (mainly legacy PFAS),[139,140] isomer fingerprints in environmental and biological samples may offer a powerful means of distinguishing between historical and later emissions.[26]

Author contributions

Mindula K. Wijayahena: conceptualization; data curation; formal analysis; investigation; methodology; validation; visualization; writing – original draft; writing – review & editing, Diana S. Aga: conceptualization, methodology; validation; writing – review & editing, visualization; funding acquisition; project administration; supervision.

Conflicts of interest

The authors declare no competing financial interest.

Data availability

No primary research results, new software or code have been included, and no new data were generated or analysed as part of this review. Web of Science, Google Scholar and general Google searches were used to obtain the papers reviewed in this paper.

Acknowledgements

The authors would like to acknowledge funding support from the US Environmental Protection Agency STAR grant (award no. 84045101). Any opinions, findings, conclusions, or recommendations expressed in this publication are those of the authors and do not necessarily reflect the views of the USEPA. The authors thank John C. Pinti for his assistance with TOC figure preparation in the manuscript and Dr. Joshua S. Wallace for valuable discussions in preparing the revised manuscript.

References

1 D. Q. Andrews, T. Stoiber, A. M. Temkin and O. V. Naidenko, *Sci. Total Environ.*, 2023, **901**, 165939.
2 Z. Wang, J. C. DeWitt, C. P. Higgins and I. T. Cousins, *Environ. Sci. Technol.*, 2017, **51**, 2508–2518.
3 M. Houde, J. W. Martin, R. J. Letcher, K. R. Solomon and D. C. G. Muir, *Environ. Sci. Technol.*, 2006, **40**, 3463–3473.
4 V. M. Vieira, K. Hoffman, H. M. Shin, J. M. Weinberg, T. F. Webster and T. Fletcher, *Environ. Health Perspect.*, 2013, **121**, 318–323.
5 R. C. Lewis, L. E. Johns and J. D. Meeker, *Int. J. Environ. Res. Public Health*, 2015, **12**, 6098–6114.
6 P. Grandjean, *Environ. Health*, 2018, **17**, 62.
7 P. Grandjean, C. A. G. Timmermann, M. Kruse, F. Nielsen, P. J. Vinholt, L. Boding, C. Heilmann and K. Molbak, *PLoS One*, 2020, **15**, e0244815.
8 K. M. Rios-Bonilla, D. S. Aga, J. Lee, M. Konig, W. Qin, J. R. Cristobal, G. E. Atilla-Gokcumen and B. I. Escher, *Environ. Sci. Technol.*, 2024, **58**, 16774–16784.
9 J. Guillen, F. Natale, N. Carvalho, J. Casey, J. Hofherr, J. N. Druon, G. Fiore, M. Gibin, A. Zanzi and J. T. Martinsohn, *Ambio*, 2019, **48**, 111–122.
10 Food and Agriculture Organization (FAO) of the United Nations. FAO Report: Global fisheries and aquaculture production reaches a new record high, https://www.fao.org/americas/news/news-detail/fao-report–global-fisheries-and-aquaculture-production-reaches-a-new-record-high/en?utm_source=chatgpt.com, (accessed February 2025).
11 U.S. Environmental, Protection Agency (EPA), Support for Fish and Shellfish Advisory Programs, https://www.epa.gov/choose-fish-and-shellfish-wisely/support-fish-and-shellfish-advisory-programs, (accessed May 2025).
12 Maine Center for Disease Control and Prevention (CDC) Scientific Brief: 2024 PFOS Fish Consumption Advisory, https://www.maine.gov/dhhs/mecdc/sites/maine.gov.dhhs.mecdc/files/pfos-fish-brunswick-08232024.pdf, (accessed March 2025).
13 N. M. Brennan, A. T. Evans, M. K. Fritz, S. A. Peak and H. E. von Holst, *Int. J. Environ. Res. Public Health*, 2021, **18**, 10900.
14 L. Teunen, L. Bervoets, C. Belpaire, M. De Jonge and T. Groffen, *Environ. Sci. Eur.*, 2021, **33**, 39.
15 G. Boisvert, C. Sonne, F. F. Riget, R. Dietz and R. J. Letcher, *Environ. Pollut.*, 2019, **252**, 1335–1343.
16 C. Vendl, M. D. Taylor, J. Bräunig, L. Ricolfi, R. Ahmed, M. Chin, M. J. Gibson, D. Hesselson, G. G. Neely, M. Lagisz and S. Nakagawa, *Ecol. Solution Evidence*, 2024, **5**, e12292.
17 Environment working group (ewg). PFAS contamination in wildlife, https://www.ewg.org/interactive-maps/pfas_in_wildlife2/map/, (accessed November 2025).
18 H. L. Walsh, V. S. Blazer, E. Lord, S. T. Hurley and D. R. LeBlanc, *Aquat. Toxicol.*, 2025, **287**, 107499.
19 R. C. Buck, J. Franklin, U. Berger, J. M. Conder, I. T. Cousins, P. de Voogt, A. A. Jensen, K. Kannan, S. A. Mabury and S. P. van Leeuwen, *Integr. Environ. Assess. Manage.*, 2011, **7**, 513–541.
20 J. Glüge, M. Scheringer, I. T. Cousins, J. C. DeWitt, G. Goldenman, D. Herzke, R. Lohmann, C. A. Ng, X. Trier and Z. Wang, *Environ. Sci.:Processes Impacts*, 2020, **22**, 2345–2373.
21 I. T. Cousins, J. H. Johansson, M. E. Salter, B. Sha and M. Scheringer, *Environ. Sci. Technol.*, 2022, **56**, 11172–11179.
22 M. G. Evich, M. J. B. Davis, J. P. McCord, B. Acrey, J. A. Awkerman, D. R. U. Knappe, A. B. Lindstrom, T. F. Speth, C. Tebes-Stevens, M. J. Strynar, Z. Wang, E. J. Weber, W. M. Henderson and J. W. Washington, *Science*, 2022, **375**, eabg9065.
23 A. O. De Silva, J. M. Armitage, T. A. Bruton, C. Dassuncao, W. Heiger-Bernays, X. C. Hu, A. Kärrman, B. Kelly, C. Ng, A. Robuck, M. Sun, T. F. Webster and E. M. Sunderland, *Environ. Toxicol. Chem.*, 2021, **40**, 631–657.
24 S. E. Fenton, A. Ducatman, A. Boobis, J. C. DeWitt, C. Lau, C. Ng, J. S. Smith and S. M. Roberts, *Environ. Toxicol. Chem.*, 2021, **40**, 606–630.
25 EPA Comptox Dashboard (USEPA. 2024. "CompTox Chemicals Dashboard." U. S. Environmental Protection Agency. https://www.epa.gov/chemical-research/comptox-chemicals-dashboard (accessed August 2024).
26 J. P. Benskin, A. O. De Silva and J. W. Martin, in *Reviews of Environmental Contamination and Toxicology, Perfluorinated alkylated substances*, ed. P. De Voogt, Springer New York, New York, NY, 2010, vol. 208, pp. 111–160, DOI: 10.1007/978-1-4419-6880-7_2.
27 A. B. Lindstrom, M. J. Strynar and E. L. Libelo, *Environ. Sci. Technol.*, 2011, **45**, 7954–7961.
28 K. Schulz, M. R. Silva and R. Klaper, *Sci. Total Environ.*, 2020, **733**, 139186.
29 V. I. Furdui, P. A. Helm, P. W. Crozier, C. Lucaciu, E. J. Reiner, C. H. Marvin, D. M. Whittle, S. A. Mabury and G. T. Tomy, *Environ. Sci. Technol.*, 2008, **42**, 4739–4744.
30 M. Chen, L. Qiang, X. Pan, S. Fang, Y. Han and L. Zhu, *Environ. Sci. Technol.*, 2015, **49**, 13817–13824.
31 H. Peng, S. Zhang, J. Sun, Z. Zhang, J. P. Giesy and J. Hu, *Environ. Sci. Technol.*, 2014, **48**, 1058–1066.
32 M. K. Wijayahena, I. S. Moreira, P. M. L. Castro, S. Dowd, M. I. Marciesky, C. Ng and D. S. Aga, *Sci. Total Environ.*, 2025, **959**, 178348.

33 Y. Yu, K. Zhang, Z. Li, C. Ren, J. Chen, Y. H. Lin, J. Liu and Y. Men, *Environ. Sci. Technol.*, 2020, **54**, 14393–14402.
34 OECD, Synthesis Report on Understanding Side-Chain Fluorinated Polymers and Their Life Cycle, OECD Series on Risk Management of Chemicals, https://one.oecd.org/document/ENV/CBC/MONO(2022)35/en/pdf, (accessed January, 2026).
35 European Environment Agency. PFAS polymers in focus: supporting Europe's zero pollution, low-carbon and circular economy ambitions, https://www.eea.europa.eu/en/analysis/publications/pfas-polymers-in-focus?activeTab=4a75727f-4f3c-4b71-bbce-9a2481c20210, (accessed January, 2026).
36 H. Jin, Y. Zhang, W. Jiang, L. Zhu and J. W. Martin, *Environ. Sci. Technol.*, 2016, **50**, 7808–7815.
37 N. Riddell, G. Arsenault, J. P. Benskin, B. Chittim, J. W. Martin, A. McAlees and R. McCrindle, *Environ. Sci. Technol.*, 2009, **43**, 7902–7908.
38 I. Gyllenhammar, J. P. Benskin, O. Sandblom, U. Berger, L. Ahrens, S. Lignell, K. Wiberg and A. Glynn, *Environ. Sci. Technol.*, 2018, **52**, 7101–7110.
39 M. K. Wijayahena, R. Kachangoon, C. Witmer, J. S. Wallace, J. Vichapong and D. S. Aga, *J. Agric. Food Chem.*, 2025, **73**, 25967–25977.
40 J. Z. Paddayuman, M. K. Wijayahena, J. M. N. Aguilar, Z. A. Gernold, J. S. Wallace and D. S. Aga, *J. Am. Soc. Mass Spectrom.*, 2025, **36**, 2470–2479.
41 S. W. C. Chung and C. H. Lam, *J. Agric. Food Chem.*, 2014, **62**, 5805–5811.
42 A. K. Greaves and R. J. Letcher, *Chemosphere*, 2013, **93**, 574–580.
43 S. Fang, R. Guo, X. Zhao and H. Jin, *Water Res.*, 2025, **271**, 122904.
44 S. Ullah, S. Huber, A. Bignert and U. Berger, *Environ. Int.*, 2014, **65**, 63–72.
45 Q. Wang, Y. Ruan, L. Jin, L. S. R. Tao, H. Lai, G. Li, L. W. Y. Yeung, K. M. Y. Leung and P. K. S. Lam, *Environ. Sci. Technol.*, 2023, **57**, 8355–8364.
46 Z. Wang, M. MacLeod, I. T. Cousins, M. Scheringer and K. Hungerbühler, *Environ. Chem.*, 2011, **8**, 389–398.
47 M. Houde, G. Czub, J. M. Small, S. Backus, X. Wang, M. Alaee and D. C. G. Muir, *Environ. Sci. Technol.*, 2008, **42**, 9397–9403.
48 A. Hanley, Method 1633, Revision A. United States Environmental Protection Agency (EPA), Water. 2024. https://www.epa.gov/system/files/documents/2024-12/method-1633a-december-5-2024-508-compliant.pdf. (accessed December 2024).
49 L. Rosenblum, Method 533, United States Environmental Protection Agency (EPA), Water. 2019. https://www.epa.gov/dwanalyticalmethods/method-533-determination-and-polyfluoroalkyl-substances-drinking-water-isotope (accessed April 2024).
50 M. Li, X.-W. Zeng, Z. Qian, M. G. Vaughn, S. Sauvé, G. Paul, S. Lin, L. Lu, L.-W. Hu, B.-Y. Yang, Y. Zhou, X.-D. Qin, S.-L. Xu, W.-W. Bao, Y.-Z. Zhang, P. Yuan, J. Wang, C. Zhang, Y.-P. Tian, M. Nian, X. Xiao, C. Fu and G.-H. Dong, *Environ. Int.*, 2017, **102**, 1–8.
51 W.-W. Bao, Z. Qian, S. D. Geiger, E. Liu, Y. Liu, S.-Q. Wang, W. R. Lawrence, B.-Y. Yang, L.-W. Hu, X.-W. Zeng and G.-H. Dong, *Sci. Total Environ.*, 2017, **607–608**, 1304–1312.
52 M. Nian, Q.-Q. Li, M. Bloom, Z. Qian, K. M. Syberg, M. G. Vaughn, S.-Q. Wang, Q. Wei, M. Zeeshan, N. Gurram, C. Chu, J. Wang, Y.-P. Tian, L.-W. Hu, K.-K. Liu, B.-Y. Yang, R.-Q. Liu, D. Feng, X.-W. Zeng and G.-H. Dong, *Environ. Res.*, 2019, **172**, 81–88.
53 J. Wang, X.-W. Zeng, M. S. Bloom, Z. Qian, L. J. Hinyard, R. Belue, S. Lin, S.-Q. Wang, Y.-P. Tian, M. Yang, C. Chu, N. Gurram, L.-W. Hu, K.-K. Liu, B.-Y. Yang, D. Feng, R.-Q. Liu and G.-H. Dong, *Chemosphere*, 2019, **218**, 1042–1049.
54 M. Zeeshan, Y. Yang, Y. Zhou, W. Huang, Z. Wang, X. Y. Zeng, R. Q. Liu, B. Y. Yang, L. W. Hu, X. W. Zeng, X. Sun, Y. Yu and G. H. Dong, *Environ. Int.*, 2020, **137**, 105555.
55 H.-S. Liu, L.-L. Wen, P.-L. Chu and C.-Y. Lin, *Environ. Pollut.*, 2018, **232**, 73–79.
56 M. Soudani, L. Hegg, C. Rime, C. Coquoz, D. B. Grosjean, F. Danza, N. Solca, F. Lucarini and D. Staedler, *Anal. Bioanal. Chem.*, 2024, **416**, 6377–6386.
57 M. Bedi, Y. Sapozhnikova, R. B. Taylor and C. Ng, *J. Hazard. Mater.*, 2023, **459**, 132062.
58 B. Ruffle, U. Vedagiri, D. Bogdan, M. Maier, C. Schwach and C. Murphy-Hagan, *Environ. Res.*, 2020, **190**, 109932.
59 W. Young, S. Wiggins, W. Limm, C. M. Fisher, L. DeJager and S. Genualdi, *J. Agric. Food Chem.*, 2022, **70**, 13545–13553.
60 C.-S. Lee, O. N. Shipley, X. Ye, N. S. Fisher, A. J. Gallagher, M. G. Frisk, B. S. Talwar, E. V. C. Schneider and A. K. Venkatesan, *Environ. Sci. Technol.*, 2024, **58**, 13087–13098.
61 A. K. Boatman, J. R. Chappel, M. E. Polera, J. N. Dodds, S. M. Belcher and E. S. Baker, *Environ. Sci. Technol.*, 2024, **58**, 14486–14495.
62 C. R. Powley, S. W. George, M. H. Russell, R. A. Hoke and R. C. Buck, *Chemosphere*, 2008, **70**, 664–672.
63 S. Balgooyen, M. Scott, B. R. Blackwell, E. L. Pulster, M. B. Mahon, R. F. Lepak and W. J. Backe, *Environ. Sci. Technol.*, 2025, **59**, 3759–3770.
64 H. Martínez-Pérez-Cejuela, M. L. Williams, C. McLeod and E. Gionfriddo, *Anal. Chim. Acta*, 2025, **1345**, 343746.
65 K. S. Kumar, Y. Zushi, S. Masunaga, M. Gilligan, C. Pride and K. S. Sajwan, *Mar. Pollut. Bull.*, 2009, **58**, 621–629.
66 R. L. Sharpe, J. P. Benskin, A. H. Laarman, S. L. MacLeod, J. W. Martin, C. S. Wong and G. G. Goss, *Environ. Toxicol. Chem.*, 2010, **29**, 1957–1966.
67 S. Fang, S. Zhao, Y. Zhang, W. Zhong and L. Zhu, *Environ. Pollut.*, 2014, **193**, 224–232.
68 A. S. Lloyd, V. A. Bailey, S. J. Hird, A. Routledge and D. B. Clarke, *Rapid Commun. Mass Spectrom.*, 2009, **23**, 2923–2938.

69 A. M. Ali, M. Sanden, C. P. Higgins, S. E. Hale, W. M. Alarif, S. S. Al-Lihaibi, E. M. Raeder, H. A. Langberg and R. Kallenborn, *Environ. Pollut.*, 2021, **280**, 116935.
70 A. M. Ali, H. A. Langberg, S. E. Hale, R. Kallenborn, W. F. Hartz, A.-K. Mortensen, T. M. Ciesielski, C. A. McDonough, B. M. Jenssen and G. D. Breedveld, *Environ. Sci.:Processes Impacts*, 2021, **23**, 588–604.
71 J. Kratzer, L. Ahrens, A. Roos, B.-M. Backlin and R. Ebinghaus, *Chemosphere*, 2011, **84**, 1592–1600.
72 B. J. Asher, Y. Wang, A. O. De Silva, S. Backus, D. C. G. Muir, C. S. Wong and J. W. Martin, *Environ. Sci. Technol.*, 2012, **46**, 7653–7660.
73 Z. Zhang, H. Peng, Y. Wan and J. Hu, *Environ. Sci. Technol.*, 2015, **49**, 1453–1461.
74 D. A. Miranda, J. P. Benskin, R. Awad, G. Lepoint, J. Leonel and V. Hatje, *Sci. Total Environ.*, 2021, **754**, 142146.
75 A. Karrman, K. Elgh-Dalgren, C. Lafossas and T. Moskeland, *Environ. Chem.*, 2011, **8**, 372–380.
76 A. Rotander, A. Karrman, B. van Bavel, A. Polder, F. Riget, G. A. Auounsson, G. Vikingsson, G. W. Gabrielsen, D. Bloch and M. Dam, *Chemosphere*, 2012, **86**, 278–285.
77 B. S. Crimmins, X. Xia, P. K. Hopke and T. M. Holsen, *Anal. Bioanal. Chem.*, 2014, **406**, 1471–1480.
78 Y. Shi, R. Vestergren, T. H. Nost, Z. Zhou and Y. Cai, *Environ. Sci. Technol.*, 2018, **52**, 4592–4600.
79 A. Koch, A. Kaerrman, L. W. Y. Yeung, M. Jonsson, L. Ahrens and T. Wang, *Environ. Sci.: Processes Impacts*, 2019, **21**, 1887–1898.
80 A. A. Aquilina-Beck, J. L. Reiner, K. W. Chung, M. J. DeLise, P. B. Key and M. E. DeLorenzo, *Arch. Environ. Contam. Toxicol.*, 2020, **79**, 333–342.
81 K. L. Hassell, T. L. Coggan, T. Cresswell, A. Kolobaric, K. Berry, N. D. Crosbie, J. Blackbeard, V. J. Pettigrove and B. O. Clarke, *Environ. Toxicol. Chem.*, 2020, **39**, 595–603.
82 R. Vestergren, S. Ullah, I. T. Cousins and U. Berger, *J. Chromatogr. A*, 2012, **1237**, 64–71.
83 S. Valsecchi, M. Rusconi and S. Polesello, *Anal. Bioanal. Chem.*, 2013, **405**, 143–157.
84 W. A. Gebbink, A. Bignert and U. Berger, *Environ. Sci. Technol.*, 2016, **50**, 6354–6362.
85 A. L. Soerensen, J. P. Benskin and S. Faxneld, *Environ. Sci. Technol.*, 2024, **58**, 10806–10816.
86 A. Koch, M. Jonsson, L. W. Y. Yeung, A. Karrman, L. Ahrens, A. Ekblad and T. Wang, *Environ. Sci. Technol.*, 2021, **55**, 7900–7909.
87 W. A. Gebbink, R. Bossi, F. F. Riget, A. Rosing-Asvid, C. Sonne and R. Dietz, *Chemosphere*, 2016, **144**, 2384–2391.
88 M. D. Malinsky, C. B. Jacoby and W. K. Reagen, *Anal. Chim. Acta*, 2011, **683**, 248–257.
89 C. J. A. F. Kwadijk, P. Korytar and A. A. Koelmans, *Environ. Sci. Technol.*, 2010, **44**, 3746–3751.
90 A. O. De Silva, D. C. G. Muir and S. A. Mabury, *Environ. Toxicol. Chem.*, 2009, **28**, 1801–1814.
91 A. O. De Silva, P. J. Tseng and S. A. Mabury, *Environ. Toxicol. Chem.*, 2009, **28**, 330–337.
92 S. Chu and R. J. Letcher, *Anal. Chem.*, 2009, **81**, 4256–4262.
93 D. Izquierdo-Sandoval, D. Fabregat-Safont, L. Lacalle-Bergeron, J. V. Sancho, F. Hernandez and T. Portoles, *Anal. Chem.*, 2022, **94**, 9040–9047.
94 J. E. Kyle, N. Aly, X. Zheng, K. E. Burnum-Johnson, R. D. Smith and E. S. Baker, *Bioanalysis*, 2018, **10**, 279–289.
95 A. K. Boatman, G. P. Kudzin, K. D. Rock, M. P. Guillette, F. Robb, S. M. Belcher and E. S. Baker, *Sci. Total Environ.*, 2025, **985**, 179760.
96 F. Menger, J. Pohl, L. Ahrens, G. Carlsson and S. Örn, *Chemosphere*, 2020, **245**, 125573.
97 A. O. De Silva and S. A. Mabury, *Environ. Sci. Technol.*, 2004, **38**, 6538–6545.
98 W. A. Gebbink and R. J. Letcher, *Environ. Sci. Technol.*, 2010, **44**, 3739–3745.
99 V. Svihlikova, D. Lankova, J. Poustka, M. Tomaniova, J. Hajslova and J. Pulkrabova, *Chemosphere*, 2015, **129**, 170–178.
100 S. Fang, Y. Zhang, S. Zhao, L. Qiang, M. Chen and L. Zhu, *Environ. Toxicol. Chem.*, 2016, **35**, 3005–3013.
101 G. Shan, Z. Wang, L. Zhou, P. Du, X. Luo, Q. Wu and L. Zhu, *Environ. Int.*, 2016, **89–90**, 62–70.
102 G. Munoz, P. Labadie, E. Geneste, P. Pardon, S. Tartu, O. Chastel and H. Budzinski, *J. Chromatogr. A*, 2017, **1513**, 107–117.
103 W. Zhong, L. Zhang, Y. Cui, M. Chen and L. Zhu, *Sci. Total Environ.*, 2019, **647**, 992–999.
104 A. Koch, M. Jonsson, L. W. Y. Yeung, A. Karrman, L. Ahrens, A. Ekblad and T. Wang, *Environ. Sci. Technol.*, 2020, **54**, 11951–11960.
105 M. Sadia, L. W. Y. Yeung and H. Fiedler, *Environ. Pollut.*, 2020, **263**, 113721.
106 X. Wang, Y. Wang, J. Li, J. Liu, Y. Zhao and Y. Wu, *Food Addit. Contam.: Part B*, 2021, **14**, 1–11.
107 G. Shan, J. Zhao, X. Sun, L. Yang, H. Wei and L. Zhu, *ACS Environ. Sci. Technol. Water*, 2022, **2**, 730–737.
108 M. Mollier, P. Bustamante, I. Martinez-Alvarez, Q. Schull, P. Labadie, H. Budzinski, Y. Cherel and A. Carravieri, *Environ. Sci. Technol.*, 2024, **58**, 6138–6148.
109 S. Genualdi, C. Srigley, W. Young and L. De Jager, *J. Agric. Food Chem.*, 2025, **73**, 16746–16753.
110 I. R. Bailes, R. A. Phillips, J. L. Barber, S. Losada, L. S. Peck, C. Green and A. J. Sweetman, *ACS Environ. Au*, 2025, **5**, 603–615.
111 W. A. Gebbink, U. Berger and I. T. Cousins, *Environ. Int.*, 2015, **74**, 160–169.
112 G. Shan, X. Chen and L. Zhu, *J. Hazard. Mater.*, 2015, **299**, 639–646.
113 A. Pacyna-Kuchta and L. Roman, *Environ. Pollut.*, 2025, **389**, 127368.
114 J. P. Benskin, A. O. De Silva, L. J. Martin, G. Arsenault, R. McCrindle, N. Riddell, S. A. Mabury and J. W. Martin, *Environ. Toxicol. Chem.*, 2009, **28**, 542–554.

115 J. P. Benskin, A. Holt and J. W. Martin, *Environ. Sci. Technol.*, 2009, **43**, 8566–8572.
116 E. L. Mills, J. M. Casselman, R. Dermott, J. D. Fitzsimons, G. Gal, K. T. Holeck, J. A. Hoyle, O. E. Johannsson, B. F. Lantry, J. C. Makarewicz, E. S. Millard, I. F. Munawar, M. Munawar, R. O'Gorman, R. W. Owens, L. G. Rudstam, T. Schaner and T. J. Stewart, *Can. J. Fish. Aquat. Sci.*, 2003, **60**, 471–490.
117 S. Fang, X. Chen, S. Zhao, Y. Zhang, W. Jiang, L. Yang and L. Zhu, *Environ. Sci. Technol.*, 2014, **48**, 2173–2182.
118 M. Sundstrom, S. C. Chang, P. E. Noker, G. S. Gorman, J. A. Hart, D. J. Ehresman, A. Bergman and J. L. Butenhoff, *Reprod. Toxicol.*, 2012, **33**, 441–451.
119 J. P. Benskin, M. G. Ikonomou, F. A. P. C. Gobas, M. B. Woudneh and J. R. Cosgrove, *Environ. Sci. Technol.*, 2012, **46**, 6505–6514.
120 M. S. Ross, C. S. Wong and J. W. Martin, *Environ. Sci. Technol.*, 2012, **46**, 3196–3203.
121 A. O. De Silva, J. P. Benskin, L. J. Martin, G. Arsenault, R. McCrindle, N. Riddell, J. W. Martin and S. A. Mabury, *Environ. Toxicol. Chem.*, 2009, **28**, 555–567.
122 J. M. O'Brien, S. W. Kennedy, S. Chu and R. J. Letcher, *Environ. Toxicol. Chem.*, 2011, **30**, 226–231.
123 Y. Zhang, S. Beesoon, L. Zhu and J. W. Martin, *Environ. Sci. Technol.*, 2013, **47**, 10619–10627.
124 M. Houde, A. O. De Silva, D. C. G. Muir and R. J. Letcher, *Environ. Sci. Technol.*, 2011, **45**, 7962–7973.
125 J. Gaillard, B. Veyrand, M. Thomas, X. Dauchy, V. Boiteux, P. Marchand, B. Le Bizec, D. Banas and C. Feidt, *Environ. Sci. Technol.*, 2017, **51**, 7658–7666.
126 J. P. Benskin, M. G. Ikonomou, F. A. P. C. Gobas, T. H. Begley, M. B. Woudneh and J. R. Cosgrove, *Environ. Sci. Technol.*, 2013, **47**, 1381–1389.
127 S. Zhang, H. Peng, D. Mu, H. Zhao and J. Hu, *Environ. Pollut.*, 2018, **234**, 821–829.
128 U. Berger, A. Glynn, K. E. Holmström, M. Berglund, E. H. Ankarberg and A. Törnkvist, *Chemosphere*, 2009, **76**, 799–804.
129 R. J. Letcher, S. Chu, M. A. McKinney, G. T. Tomy, C. Sonne and R. Dietz, *Chemosphere*, 2014, **112**, 225–231.
130 X. Ma, G. Shan, M. Chen, J. Zhao and L. Zhu, *Sci. Total Environ.*, 2018, **612**, 18–25.
131 H. Peng, Q. Wei, Y. Wan, J. P. Giesy, L. Li and J. Hu, *Environ. Sci. Technol.*, 2010, **44**, 1868–1874.
132 C. M. Butt, D. C. G. Muir, I. Stirling, M. Kwan and S. A. Mabury, *Environ. Sci. Technol.*, 2007, **41**, 42–49.
133 D. A. Ellis, J. W. Martin, A. O. De Silva, S. A. Mabury, M. D. Hurley, M. P. S. Andersen and T. J. Wallington, *Environ. Sci. Technol.*, 2004, **38**, 3316–3321.
134 M. J. A. Dinglasan, Y. Ye, E. A. Edwards and S. A. Mabury, *Environ. Sci. Technol.*, 2004, **38**, 2857–2864.
135 L. Zhao, F. Chen, F. Guo, W. Liu and K. Liu, *Chirality*, 2019, **31**, 870–878.
136 E. F. Houtz, C. P. Higgins, J. A. Field and D. L. Sedlak, *Environ. Sci. Technol.*, 2013, **47**, 8187–8195.
137 N. T. Joseph, T. Schwichtenberg, D. Cao, G. D. Jones, A. E. Rodowa, M. A. Barlaz, J. A. Charbonnet, C. P. Higgins, J. A. Field and D. E. Helbling, *Environ. Sci. Technol.*, 2023, **57**, 14351–14362.
138 M. J. Benotti, L. A. Fernandez, G. F. Peaslee, G. S. Douglas, A. D. Uhler and S. Emsbo-Mattingly, *Environ. Forensics*, 2020, **21**, 319–333.
139 American Chemical Council. PFAS Stewardship and Regulation, https://www.americanchemistry.com/chemistry-in-america/chemistries/fluorotechnology-per-and-poly-fluoroalkyl-substances-pfas/pfas-stewardship-and-regulation, (accessed November, 2025).
140 EPA and 3M announce phase out of PFOS, https://www.epa.gov/archive/epapages/newsroom_archive/newsreleases/33aa946e6cb11f35852568e1005246b4.html, (accessed November, 2025).